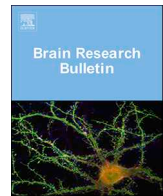




ELSEVIER

Contents lists available at ScienceDirect

Brain Research Bulletin

journal homepage: www.elsevier.com/locate/brainresbull

Research report

Potential role of P2X7 receptor in neurodegenerative processes in a murine model of glaucoma

María J. Pérez de Lara^a, Marcelino Avilés-Trigueros^b, Ana Guzmán-Aránguez^a,
F. Javier Valiente-Soriano^b, Pedro de la Villa^c, Manuel Vidal-Sanz^{b,*}, Jesús Pintor^a

^a Department of Biochemistry and Molecular Biology IV, Faculty of Optics and Optometry, Complutense University of Madrid, c/Arcos de Jalón 118, E-28037, Madrid, Spain

^b Laboratory of Experimental Ophthalmology, Dept. of Ophthalmology, Faculty of Medicine, University of Murcia and Murcia Institute of Bio-Health Research (IMIB), E-30120, El Palmar, Murcia, Spain

^c Systems Biology Department, Faculty of Medicine, University of Alcalá, Alcalá de Henares, Madrid, Spain

ARTICLE INFO

Keywords:

Glaucoma
Retinal ganglion cells (RGC)
Neuronal degeneration
Apoptosis
Electroretinogram (ERG)
P2X7
MAPK

ABSTRACT

Glaucoma is a common cause of visual impairment and blindness, characterized by retinal ganglion cell (RGC) death. The mechanisms that trigger the development of glaucoma remain unknown and have gained significant relevance in the study of this neurodegenerative disease. P2X7 purinergic receptors (P2X7R) could be involved in the regulation of the synaptic transmission and neuronal death in the retina through different pathways. The aim of this study was to characterize the molecular signals underlying glaucomatous retinal injury.

The time-course of functional, morphological, and molecular changes in the glaucomatous retina of the DBA/2J mice were investigated. The expression and localization of P2X7R was analysed in relation with retinal markers. Caspase-3, JNK, and p38 were evaluated in control and glaucomatous mice by immunohistochemical and western-blot analysis. Furthermore, electroretinogram recordings (ERG) were performed to assess inner retina dysfunction.

Glaucomatous mice exhibited changes in P2X7R expression as long as the pathology progressed. There was P2X7R overexpression in RGCs, the primary injured neurons, which correlated with the loss of function through ERG measurements. All analyzed MAPK and caspase-3 proteins were upregulated in the DBA/2J retinas suggesting a pro-apoptotic cell death.

The increase in P2X7Rs presence may contribute, together with other factors, to the changes in retinal functionality and the concomitant death of RGCs. These findings provide evidence of possible intracellular pathways responsible for apoptosis regulation during glaucomatous degeneration.

1. Introduction

Glaucoma is a neurodegenerative disease characterized by optic nerve degeneration and retinal ganglion cell (RGC) death (Quigley and Broman, 2006; Schlamp et al., 2006; Howell et al., 2007). It is often correlated with an elevated intraocular pressure (IOP) (Schuettauf et al., 2004; Salinas-Navarro et al., 2009; Cuenca et al., 2010; Salinas-Navarro et al., 2010). RGC injury during glaucomatous optic neuropathy development is one of the main reasons that lead to blindness, this being originated by the contribution of several factors. In this sense, glutamate-induced excitotoxicity (Casson, 2006), hypoxic insult, neurotrophic deprivation (Johnson et al., 2009) and oxidative stress (Tezel, 2006; McElnea et al., 2011; Goyal et al., 2014) play additional roles in

the pathogenesis of glaucoma. These insults have pointed to cell death by apoptotic processes (Jakobs et al., 2005; Zhou et al., 2005). Programmed cell death can contribute to RGC loss in different models of glaucoma (Sawada and Neufeld, 1999; Ko et al., 2000; Tatton et al., 2001; Zhang et al., 2005) and optic nerve transection (Agudo et al., 2008, 2009; Levkovitch-Verbin et al., 2013; Levkovitch-Verbin, 2015; Sanchez-Migallon et al., 2016, 2018). Markers of apoptosis have also been observed in the human glaucomatous retina (Kerrigan et al., 1997; Okisaka et al., 1997).

There is compelling evidence that purinergic receptors have an important role in ocular structures. The P2X7 receptor (P2X7R) is a ligand-gated ion channel that belongs to P2X purinergic receptors family. The P2X7 is activated by low concentrations of extracellular ATP

* Corresponding author at: Department of Ophthalmology, Faculty of Medicine, University of Murcia, Edificio Departamental, 5ª Planta, Campus de CC de la Salud, E-30129, El Palmar, Murcia, Spain.

E-mail address: manuel.vidal@um.es (M. Vidal-Sanz).

<https://doi.org/10.1016/j.brainresbull.2019.05.006>

Received 28 August 2018; Received in revised form 23 April 2019; Accepted 10 May 2019

Available online 16 May 2019

0361-9230/© 2019 The Authors. Published by Elsevier Inc. This is an open access article under the CC BY license

(<http://creativecommons.org/licenses/by/4.0/>).

(Surprenant et al., 1996). Its prolonged activation elicits the opening of a transmembrane pore, permeable to large molecular weight molecules which finally leads to cellular death (Di Virgilio et al., 1998). The P2X7R has been detected in neurons (Wheeler-Schilling et al., 2001; Ishii et al., 2003; Puthussery and Fletcher, 2004; Puthussery et al., 2006; Vessey and Fletcher, 2012), microglial cells (Franke et al., 2005; Vessey and Fletcher, 2012), and astrocytes (Vessey and Fletcher, 2012) from rodent and primate retina.

The P2X7R is expressed in different layers in the retina and has been implicated in neurodegenerative diseases including neuroimmune and neuroinflammatory reactions (Skaper et al., 2010; Weisman et al., 2012; Catanzaro et al., 2014). Electrophysiological, pharmacological and immunological studies evidence the presence and the role of P2X7 in neuronal functions and injury. Several studies have demonstrated the involvement of P2X7R in retinal impairment. Increased levels of ATP and P2X7R activation were observed in hypertensive models of glaucomatous damage in *in vitro* (Resta et al., 2005; Reigada et al., 2008; Hu et al., 2010; Xia et al., 2012) and *in vivo* models (Zhang et al., 2007; Li et al., 2011; Niyadurupola et al., 2013; Sugiyama et al., 2013). Furthermore, P2X7R activation may also be associated with hypoxia-induced death of retinal neurons (Sugiyama et al., 2010) and retinitis pigmentosa model (Franke et al., 2005).

Stimulation of P2X7R is involved in the modulation of neuronal retinal neurotransmission (Puthussery et al., 2006) and neuronal death (Franke et al., 2005) in murine models and in primary retinal cultures (Resta et al., 2005; Reigada et al., 2008; Hu et al., 2010; Sugiyama et al., 2010). Furthermore, this stimulation increases protein tyrosine phosphorylation (Adinolfi et al., 2003; Aga et al., 2004) leading to MAPK pathway activation, proteins which have a determinant role in the commitments of the cells to apoptosis (Panenka et al., 2001; Wang et al., 2003; Kong et al., 2005). Due to these findings, recent studies suggest a protective role of the P2X7R antagonists (Di Virgilio et al., 2001; Franke et al., 2004; Jun et al., 2007; Diaz-Hernandez et al., 2009).

An interesting model of glaucoma where the retinal changes and the participation of P2X7 receptors can be studied is the DBA/2J mouse. This is a well-established model for secondary angle-closure glaucoma (Jakobs et al., 2005; Anderson et al., 2006), caused by mutations in the *Gpnmb* and *Tyrp* genes (John et al., 1998; Anderson et al., 2002; Libby et al., 2005; Anderson et al., 2006; Howell et al., 2007). DBA/2J presents a gradual increase in IOP, which is maximal between the 9th and 12th month of age (Anderson et al., 2002). This rise in the IOP is mainly due to the iris pigment dispersion in the eye anterior chamber produced by iris atrophy (Anderson et al., 2002). The rise in IOP might be the key factor that produces retinal cell damage in this animal model (Inman et al., 2006). Interestingly, retinal cell death will concomitantly produce a visual dysfunction that can be recorded by electroretinography (Alarcon-Martinez et al., 2009; Salinas-Navarro et al., 2009; Cuenca et al., 2010; Montalban-Soler et al., 2012; Perez de Lara et al., 2014; Smith et al., 2014).

In this sense, the present study focused on the characterization of a murine spontaneous model of glaucoma, the DBA/2J, and the possible role of activated/up-regulated P2X7R by ATP in RGC death during the development of the pathology. To understand the RGC death mechanism we investigated whether the activated apoptotic cascades in RGC death were associated with alterations in the activation of mitogen-activated protein kinases (MAPK) signaling pathways.

2. Materials and methods

2.1. Animal handling

The experiments were performed on female DBA/2J (n = 26) and C57BL/6J (n = 26) mice obtained from the European distributor of the Jackson Laboratories (Charles Rivers Laboratories). All animal maintenance and experimental procedures followed in compliance with

institutional, Spanish and European guidelines of animal care in the laboratory and animal research (Guide for the Care and Use of Laboratory Animals) and the ARVO Statement for the Use of Animals in Ophthalmic and Vision Research. All animal studies were performed with authorization of the institutional Animal Care and Use Committee from the Complutense University of Madrid (Spain). Four mice were housed per cage in temperature and light-controlled rooms maintained on a 12 h light/dark cycle, and all animals had access to food and water *ad libitum*. DBA/2J and C57BL/6J mice were studied at 3 and 15 months. C57BL/6J mice were used as control.

For ERG measurements, mice were weighted and anesthetized with an intraperitoneal (i.p.) injection of a mixture of ketamine (95 mg/kg, Imalgene 1000[®], Merial Laboratorios, S.A., Barcelona, Spain) and xylazine (5 mg/kg, Rompun[®], Bayer, S.A, Barcelona, Spain). While recovering from anesthesia, mice were placed in their cages, and an ocular ointment containing neomycin and prednisone (Oftalmolosa Cusi Prednisona-Neomicina[®]; Alcon S.A., Barcelona, Spain) was applied on the cornea to prevent corneal desiccation. Animals were euthanized with an i.p. injection of an overdose of 20% sodium pentobarbital (Dolethal[®]; Vetoquinol Especialidades Veterinarias, S.A., Alcobendas, Madrid, Spain).

The DBA/2J mice were genotyped by PCR on the tail DNA (Mangiarini et al., 1996) to assure the presence the mutations in *Tyrp1* and *Gpnmb* genes (data not shown) (Perez de Lara et al., 2014).

2.2. Electroretinogram recordings

The mice (n = 12 mice for each group) were adapted to darkness overnight before electroretinogram recordings (ERG), and all manipulation procedures were performed under dim red light ($\lambda > 600$ nm). Anaesthesia was induced by i.p. injection of a mixture of ketamine and xylazine in saline (see above) and kept on a heating pad to maintain normal body temperature at 37 °C. Pupil mydriasis was induced by applying a topical drop of 1% tropicamide (Colircusí Tropicamide 1%[®]; Alcon-Cusí, S.A., El Masnou, Barcelona, Spain) in the right eye of the experimental animal before placing the corneal electrode. The recording system comprised Burian-Allen lens electrodes (Hansen Labs, Coralville, Iowa, USA) positioned on the cornea. The corneal surface had been previously protected with a drop of methylcellulose (Methocel 2%[®]; Novartis Laboratories CIBA Vision, Annonay, France) to maximize conductivity. The reference electrode was placed in the mouth, and the ground electrode was inserted subcutaneously at the base of the tail. After positioning the electrodes, the mice resting on the warming pad were placed in a Ganzfeld stimulator. Flash-induced ERG stimulation was provided by a Ganzfeld dome light source, which ensured a uniform illumination of the retina and provided a wide range of light intensities. Electrical signals generated in the retina were amplified (x1000) and band filtered between 0.3 and 1000 Hz, using an amplifier (CP511 AC amplifier; Grass Instruments, Quincy, MA). Electrical signals were digitized at 20 kHz, using a data acquisition board (PowerLab; AD Instruments, Chalgrove, UK) and displayed on a PC computer monitor. Light stimuli were calibrated periodically with a photometer (Mavo Monitor USB, Gossen, Nürenberg, Germany). The scotopic responses elicited by stimulation of the retina with light intensities increasing from 10^{-5} to 10^{-2} cd·s·m⁻² were recorded in the right eye to determine the Scotopic Threshold Response (STR). A series of ERG responses were averaged (≈ 20 ERGs for each trace) for each light intensity, after adjusting the time interval between flashes to ensure complete recovery of the response (10 s for the dimmest stimulus intensities and 30 s for the strongest stimuli). Standard ERG waves were analyzed according to the method recommended by the International Society for Clinical Electrophysiology of Vision (ISCEV).

2.2.1. Analysis and statistics

For the statistical analysis, the positive scotopic threshold response (pSTR) was measured from the baseline to the peak of the positive

deflection (110–120 ms after the flash onset), whereas the negative scotopic threshold response (nSTR) was measured from the baseline to the peak of the negative deflection after the pSTR (approximately 220 ms from the flash onset). The C57BL/6J and DBA/2J recordings were compared at different ages for each light stimulus using GraphPad InStat[®] 3 for Windows[®] (GraphPad Software, San Diego California USA,). Descriptive statistics were calculated and the normality of the distribution of the data was examined. The Student's *t*-test was applied to compare the averaged differences (mean \pm SEM) of ERG responses of the right eyes at $-3.69 \log \text{ cd}\cdot\text{s}\cdot\text{m}^{-2}$ in both groups at different ages. Values were considered statistically significant when $p < 0.05$ for all tests.

2.3. Morphological study

A subpopulation of the animals used to study the ERG changes related with the age were used in the immunohistochemical study. C57BL/6J and DBA/2J mice at 3 and 15 months ($n = 12$ mice for each group) were deeply anesthetized, the orientation of the eyes was preserved by a suture stitch placed on the superior pole, and were perfused transcardially with 0.1 M phosphate buffer saline (PBS; pH 7.2–7.4) followed by a fixative solution of 4% paraformaldehyde in 0.1 M phosphate buffer (PB; pH 7.2–7.4) at 4 °C. The eyes were enucleated and immersed in the same fixative solution for 1 h at 4 °C. The anterior segment and the lens were removed and the eyecups were post-fixed for 30 min. at 4 °C and rinsed in PBS.

For retinal whole-mount studies both retinas were dissected out and prepared as flatten whole-mount by making four radial cuts in each retinal pole (the deepest in the superior pole) as previously described (Lindqvist et al., 2004; Salinas-Navarro et al., 2009; Galindo-Romero et al., 2011; Perez de Lara et al., 2014; Valiente-Soriano et al., 2015).

To identify the expression of P2X7 and NF in the retina at the time of animal sacrifice a simultaneous double immunostaining was performed using a rabbit polyclonal anti-P2X7 receptor (Alomone Labs) and a mouse monoclonal anti-pNFH (Serotec) at the working dilution indicated in Table 1. Retinas were pre-incubated in a blocking solution of 2% Triton X-100 in PBS containing 2% normal serum from the species that the secondary antibodies were raised in (goat and donkey, see Table 1), for 1 h at RT. Incubation with both primary antibodies was carried out in blocking solution overnight at 4 °C. After gentle rinse with 0.1% Triton X-100 in PBS, retinas were incubated with a mix of both secondary antibodies diluted 1:500 in blocking solution for 1 h at RT. After rinsing with 0.1% Triton X-100 in PBS, retinas were flat mounted on slides with the vitreal side up and covered with antifading mounting media containing 50% glycerol and 0.04% p-phenylenediamine in 0.1 M sodium carbonate buffer (pH 9.0).

Retinas were examined and photographed under a fluorescence microscope (Axioscop 2 Plus; Zeiss Mikroskopie, Jena, Germany) equipped with a fluorescein (BP 450/490, LP 515-565) and a rhodamine (BP 546/12, LP590) filter to observe the secondary Alexa Fluor[®]-488 or -568 conjugated antibodies (donkey anti rabbit and goat anti

mouse, respectively). The microscope was also equipped with a digital high-resolution camera (ProgRes[™] C10^{plus}; Jenoptik, Jena, Germany) and a computer-driven motorized stage (ProScan[™] H128 Series; Prior Scientific Instruments, Cambridge, UK) connected to image analysis software (Image-Pro Plus 5.1 for Windows (IPP); Media Cybernetics, Silver Spring, MD, USA) through a microscope controller module (Scope-Pro 5.0 for Windows; Media Cybernetics, Silver Spring, MD, USA). Retinal whole-mount reconstructions were carried out following previously described procedures (Vidal-Sanz et al., 2015, 2017). For retinal cross section studies, after rinsing in PBS the eyecups were immersed in graded sucrose in PBS (11% and 33%) for cryoprotection at 4 °C. Eyecups were oriented to get vertical sections by embedding in tissue freezing medium (Tissue-Tek[®] OCT[™] Compound; Sakura[®] Finetek Europe, B.V. Alphen van den Rijn, The Netherlands), frozen in 2-methylbutane (Sigma-Aldrich Quimica SL, Madrid, Spain) cooled with liquid nitrogen and 10 μm frozen sections were obtained on a cryostat (Microm, Walldorf, Germany). Sections were collected on poly-L-lysine coated slides and stored at -20 °C until use.

For single or double immunofluorescence studies, slices were thawed and permeabilized with 0.25% Triton X-100 in PBS for 30 min, followed by pre-incubation with the blocking solution, containing 10% normal donkey serum (NDS; Jackson ImmunoResearch, West Grove, PA, USA), 10% normal goat serum (NGS; Jackson ImmunoResearch), and 0.1% Triton X-100 in PBS for 1 h at room temperature. The slices were incubated with the primary antibodies (see Table 1) diluted in PBS-0.1% Tx-100 and 1% normal donkey or goat serum (depending on the species of the secondary antibody) overnight at 4 °C. All primary antibodies utilized in this study have been used previously in the rodent retina (Pannicke et al., 2000; Munemasa et al., 2005; Barhoum et al., 2008; Nadal-Nicolas et al., 2009; Parrilla-Reverter et al., 2009; Donovan et al., 2011; Diaz-Hernandez et al., 2012). Finally, sections were washed in PBS-0.1% Tx-100 and incubated with respective secondary antibodies diluted in PBS-0.1% Tx-100, for 1 h, in darkness at RT. Secondary antibodies used were Cy3-conjugated donkey anti-rabbit IgG(H + L) (1:200) or FITC-conjugated donkey anti-rabbit IgG(H + L) (1:200) and FITC-conjugated donkey anti-mouse IgG (H + L) (Jackson ImmunoResearch). Subsequently, sections were rinsed in PBS and mounted in antifade mounting medium (Vectashield[®]; Vector Laboratories, Burlingame, CA, USA).

Sections were examined and photographed under a confocal microscope (Zeiss LSM 5 Zeiss Mikroskopie, Jena, Germany) equipped with an argon laser (458/488/514 nm) and a helium-neon laser (543 nm). The microscope was also equipped with a digital high-resolution camera (ProgRes[™] C10^{plus}; Jenoptik, Jena, Germany) and a computer-driven motorized stage (ProScan[™] H128 Series; Prior Scientific Instruments, Cambridge, UK) connected to image analysis software. Images were collected with a resolution of 512×512 pixels ($250 \times 250 \mu\text{m}$) and projections of four frames using the single or the multi-track scanning module. Images acquired were processed using Adobe Photoshop 8.0 software (Adobe Systems, Inc., San Jose, CA, USA).

Table 1

Primary antibodies.

Molecular marker	Antibody	IH dilution	WB dilution	Source
P2X7 receptor	Rabbit polyclonal	1:200	1:1000	Alomone, APR-004
Glial fibrillary acidic protein (GFAP)	Mouse, clone G-A-5	1:200	1:400	Sigma, G3893
Synaptophysin	Mouse, clone VP-38	1:200	1:2000	Sigma, S5768
Brn3a	Goat polyclonal	1:500	1:500	Santa Cruz sc 31984
JNK1/JNK2 (phospho-Thr183/Tyr185)	Rabbit polyclonal	–	1:500	Signalway Antibody #11504
SAPK/JNK	Rabbit polyclonal	–	1:500	Cell Signaling #9252
Phospho-p38 MAP Kinase (Thr180/Tyr182))	Rabbit polyclonal	–	1:500	Cell Signaling #9211
p38 MAP Kinase	Rabbit polyclonal	–	1:500	Cell Signaling#9212
Cleaved Caspase-3 (Asp175)	Rabbit polyclonal	–	1:500	Cell Signaling #9661
Glyceraldehyde 3 phosphate dehydrogenase (GAPDH)	Rabbit polyclonal	–	1:2500	Abcam Ab9485
Glyceraldehyde 3 phosphate dehydrogenase (GAPDH)	Rabbit polyclonal	–	1:500	Santa Cruz sc166574

2.4. Quantification of ganglion cell loss

Confocal images sections were obtained using 40x magnification in glaucomatous mice and their respective control mice. Sections stained with antibody against Brn3a at different ages (3 and 15 months) were used to quantify the number of remained RGCs. All measurements were analysed in several retinal regions (central and peripheral areas) of at least 4 mice in seven captured micrographs from each eye and age point. Images were processed with the NIH ImageJ 1.42 software (Schneider et al., 2012) to perform morphometric analysis of the confocal images; the quantification of RGCs was done manually using the cell counter plugin.

2.5. Western blot analysis

Western blot experiments were performed using control and injured retinas at different stages of age, 3 and 15 months ($n = 10$ mice for each group). Samples were thawed and homogenized in lysis buffer (1% Nonidet P-40, 0.1% SDS, 0.5% deoxycolic acid, 0.15 M NaCl in 0.05 M Tris–HCl buffer, pH 8.0) supplemented with protease inhibitors (1 mM PMSF, 10 $\mu\text{g}/\text{mL}$ leupeptin, 5 $\mu\text{g}/\text{mL}$ pepstatin, 10 $\mu\text{g}/\text{mL}$ aprotinin, 1 mM sodium fluoride and 2 mM sodium orthovanadate). Tissue extracts were incubated for 30 min on ice and centrifuged at 15,000 rpm for 15 min at 4 °C. Protein concentration was quantified spectrophotometrically using the Bradford assay (Quickstart Bradford Dye Reagent 1x, Bio-Rad Laboratories, Alcobendas, Madrid, Spain). Retinal extracts (30–150 μg depending of the analyzed protein) were re-suspended in 2x Laemmli's sample buffer (glycerol, SDS, 2-mercaptoethanol, bromophenol blue in Tris–HCl buffer) at a 4:1 ratio and were loaded on a 10% SDS-polyacrilamide gel and transferred to nitrocellulose membrane (Hybond-P PVDF membranes, GE Healthcare Life Science, Germany). Blots were washed and blocked with 5% non-fat dry milk in TBS buffer (Tris–HCl, NaCl, 0.1% Tween 20) for 1 h at room temperature and were incubated overnight at 4 °C with every one of the different commercial antibodies (see Table 1). Horseradish peroxidase-conjugated secondary antibodies (Jackson ImmunoResearch, West Grove, PA, USA) at a 1:10,000 dilution for 1 h at room temperature were used. Detection was performed using an enhanced chemiluminescence system (ECL, Amersham Pharmacia Biotech). Mouse monoclonal glyceraldehyde-3-phosphate dehydrogenase (anti-GAPDH), and JNK or p38 polyclonal antibodies served as a loading control.

Films from western blots were digitized with Gel Logic 200 Imaging System (Kodak, Rochester, NY, USA). Densitometric quantitation of protein bands was accomplished using Kodak Molecular Imaging software (Kodak, Rochester, NY, USA) and values obtained for each protein were normalized to respective densitometric GAPDH or total protein (JNK and p38) in signaling pathways to check that all wells were loaded with the same amount of protein. For each quantified protein the results of at least three independent experiments were analyzed, each containing a minimum of two biological replicates.

2.6. RNA isolation and reverse transcriptase-PCR

Total RNA was isolated from the glaucomatous and control retinas at 3 and 15 months of age ($n = 4$ mice for each group) using the Nucleospin RNA/Protein Kit (Macherey-Nagel, Düren, Germany) according to the instructions of the manufacturer and 250 ng was reverse transcribed using SuperScript[®] III First-Strand synthesis system Kit (Invitrogen, Thermo Fisher Scientific, Waltham, MA USA).

The P2X7-specific primers (forward 5'-GCACGAATTATGGCACC GTC-3' and reverse 5'-ACACCTGCCAGTCTGGATTCCCT-3') that have been previously described (Sanchez-Nogueiro et al., 2005) were employed for amplification of P2X7. Glyceraldehyde-3 phosphate dehydrogenase (GAPDH) was used as an internal control and GAPDH-specific primers (forward 5'-ACCACAGTCCATGCCATCAC-3' and reverse 5'-TCCACCACCTGTTGTGTA-3') were purchased from Clontech

(Clontech, Mountain View, CA, USA). Reactions were performed using TITANUM[™] Taq DNA polymerase (Takara Bio Inc., Japan). For P2X7 amplification, reaction conditions were 95 °C for 3 min, followed by 35 cycles at 95 °C for 1 min, 68 °C for 1 min, 72 °C for 1 min and finally 72 °C for 3 min. The thermal cycling conditions for GAPDH amplification were 95 °C for 5 min, followed by 30 cycles at 95 °C for 45 s, 60 °C for 45 s, 72 °C for 2 min and 72 °C for 7 min.

PCR products were separated by electrophoresis on 1.5% agarose gel, stained by ethidium bromide and quantified using a Kodak GL 200 Imaging system and Kodak Molecular Imaging software (Kodak, Rochester, NY, USA).

2.7. Measurement of caspase-3 activity

Caspase-3 activity was determined by Caspase-3 Fluorescence Assay Kit (Cayman Chemical Company Ann Arbor, MI, USA). DBA/2J and C57BL/6J retinas were dissected from the enucleated eyes at 3 or 15 months ($n = 4$ mice for each group). Extra-caution was paid to avoid damaging the retinas as a prior step to place them in cold PBS to wash the samples. The tissue was homogenized in a lysis buffer (50 mM HEPES, pH 7.4, 100 mM NaCl, 0.1% 3-[(3-cholamidopropyl) dimethylammonio]-1-propanesulfonate, 10 mM DTT, and 100 mM EDTA, 10 $\mu\text{g}/\text{mL}$ of leupeptin, 2 $\mu\text{g}/\text{mL}$ pepstatin, 2 $\mu\text{g}/\text{mL}$ aprotinin, 1 mM PMSF, and 0.03% digitonin on ice for 30 min. The samples were centrifuged at 15,000g for 15 min at 4 °C and supernatants were transferred to an individual well of a 96-well plate. Cell lysates were tested with different dilutions and incubated with 100 μl of caspase-3 N-DEVD-N'-morpholinecarbonyl-rhodamine 110 substrate (Ac-DEVD-N'-MC-R110; Peptide Institute, Osaka, Japan). Caspase-3 was assessed by measuring the cleavage of fluorogenic substrate and was monitored by measuring excitation at 485 nm and emission at 535 nm on a plate reader (Fluoroscan Imaging Systems, Bedford, MA) over time. The arbitrary values were presented as the mean \pm SEM of three experiments with DBA/2J and control samples.

2.8. Statistical analysis

Quantitative results of morphometric analyses were analyzed by statistical software (GraphPad Prism[®] 7; GraphPad Software, Inc., La Jolla, CA, USA). For statistical studies, Student's *t*-test was performed to compare the number of RGC found at each age-point compared with control mice retinas. All analyzed images were captured in the same regions of the retina (from the peripheral to middle-central retina) to assure the suitable count of cells.

The amount of protein or mRNA presents in each spot was measured with densitometry by integration of the optical density over the spot's area. Numerical data were processed by a spreadsheet (Microsoft Excel), and statistical analyses were carried out using InStat 3 software (GraphPad Software). Statistical comparisons at different age stages between the glaucomatous and control strains were performed using the Student's *t*-test with a confidence interval of 95% followed to Wilcoxon's test or one way ANOVA test followed by Bonferroni test correction to determine statistical significance.

Statistical comparisons of protein expression in glaucomatous and control mice were performed using Student's *t*-test with a confidence interval of 95% with Welch correction followed to Kolmogorov-Smirnov method using InStat 3 software (GraphPad Software).

3. Results

3.1. Assessment of retinal function in glaucomatous mice

To determine possible electrophysiological deficits during the development of glaucomatous degeneration, the scotopic threshold response (STR) of the ERG was assessed in DBA/2J and control mice. ERG recordings were obtained at 3 and 15 months of age from right eyes in

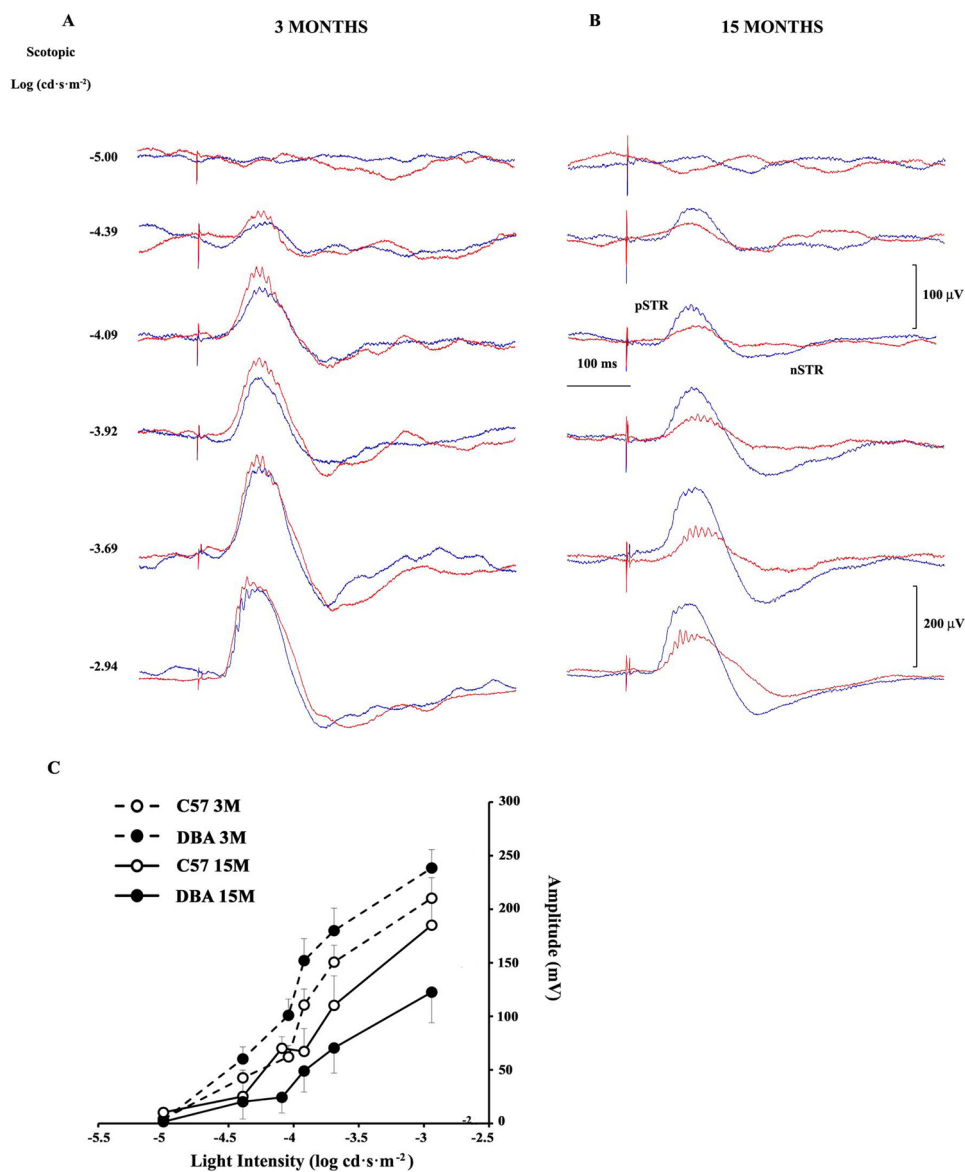


Fig. 1. Scotopic representative ERG responses recorded from control (blue traces) and glaucomatous (red traces) mice in response to flash stimuli of increasing intensity (A–B). The ERG responses were elicited by weak light stimuli from -2.94 to -5.00 log $\text{cd}\cdot\text{s}\cdot\text{m}^{-2}$. A significant reduction was observed in DBA/2J mice at 15 months comparing with the control mice. (C) pSTR response as a function of stimulus light intensity from C57BL/6J and DBA/2J at 3 and 15 months. Plot data correspond to mean values \pm SD ($n = 12$). A significant reduction in pSTR amplitude can be observed in DBA/2J between 3 and 15 months of age ($p < 0.001$) and when compared with control mice at 15 months ($p < 0.001$).

12 DBA/2J and in 12 C57BL/6J control mice. The amplitudes of positive STR (pSTR) and negative STR (nSTR) increased exponentially, in both control and glaucomatous mice as the intensity of the light stimuli increased (Fig. 1). A decrease in the magnitude of pSTR was observed in the responses of DBA/2J mice during the progress of the pathology. Fig. 1 shows representative traces of the ERG recorded in response to flash stimuli of increasing intensity ranging from -5.00 to -2.94 log $\text{cd}\cdot\text{s}\cdot\text{m}^{-2}$ in DBA/2J and C57BL/6J mice, respectively. Statistically significant differences were observed between 15 months glaucomatous and 3 months glaucomatous and control group. The pSTR trace amplitudes in DBA/2J mice decreased at 15 months of age by 52.7%, with a 95% confidence interval (t -test; $p < 0.001$). STR recordings from control mice showed no significant differences in the amplitudes of the pSTR during aging. These data suggest that this significant dysfunction of the inner retina may be correlated by a neuronal death progress.

3.2. Increase of P2X7 receptor levels in retina of DBA/2J mice

P2X7 immunoreactivity was evaluated in vertical cryostat sections of the mice retinas. The P2X7R was detected in the outer (OPL) and inner (IPL) plexiform layers, inner nuclear layer (INL) and ganglion cell layer (GCL) (Fig. 2 A–C) confirming previous reports. The distribution

pattern of P2X7 immunostaining was similar in younger mice of both strains (C57BL/6J and DBA/2J at 3 months). The glaucomatous mice retinas displayed significant increased immunoreactivity levels for the P2X7R at 15 months. Strong punctate immunoreactivity was observed in the GCL, IPL, and OPL (Fig. 2C). The P2X7R immunolabeling was measured carefully in GCL to demonstrate the protein increase in these neurons (Fig. 2A–C). Depending on the histological section, it was found a lack of RGCs (Fig. 2C) or the remaining RGCs with a strong P2X7 immunoreactivity (Fig. 2D). To quantify the up-regulation of P2X7 receptors, the level of this protein was analyzed by western blot in control and glaucomatous retinas. P2X7 receptor levels were increased (78%, $p < 0.0005$) in 15 months old DBA/2J mice, when compared to control mice (Fig. 2F). A significant increased level was observed comparing normal and glaucomatous mice at 3 months of age (36%, $p < 0.0005$).

Using RT-PCR, mRNA P2X7 levels in both strains at different ages were analyzed (Fig. 2G). Increased mRNA levels were detected in DBA/2J mice at 15 months (70%, $p < 0.005$) as compared to the control mice at the same age and DBA/2J or control mice at 3 months old. This finding is in agreement with western blot and immunohistochemistry results.

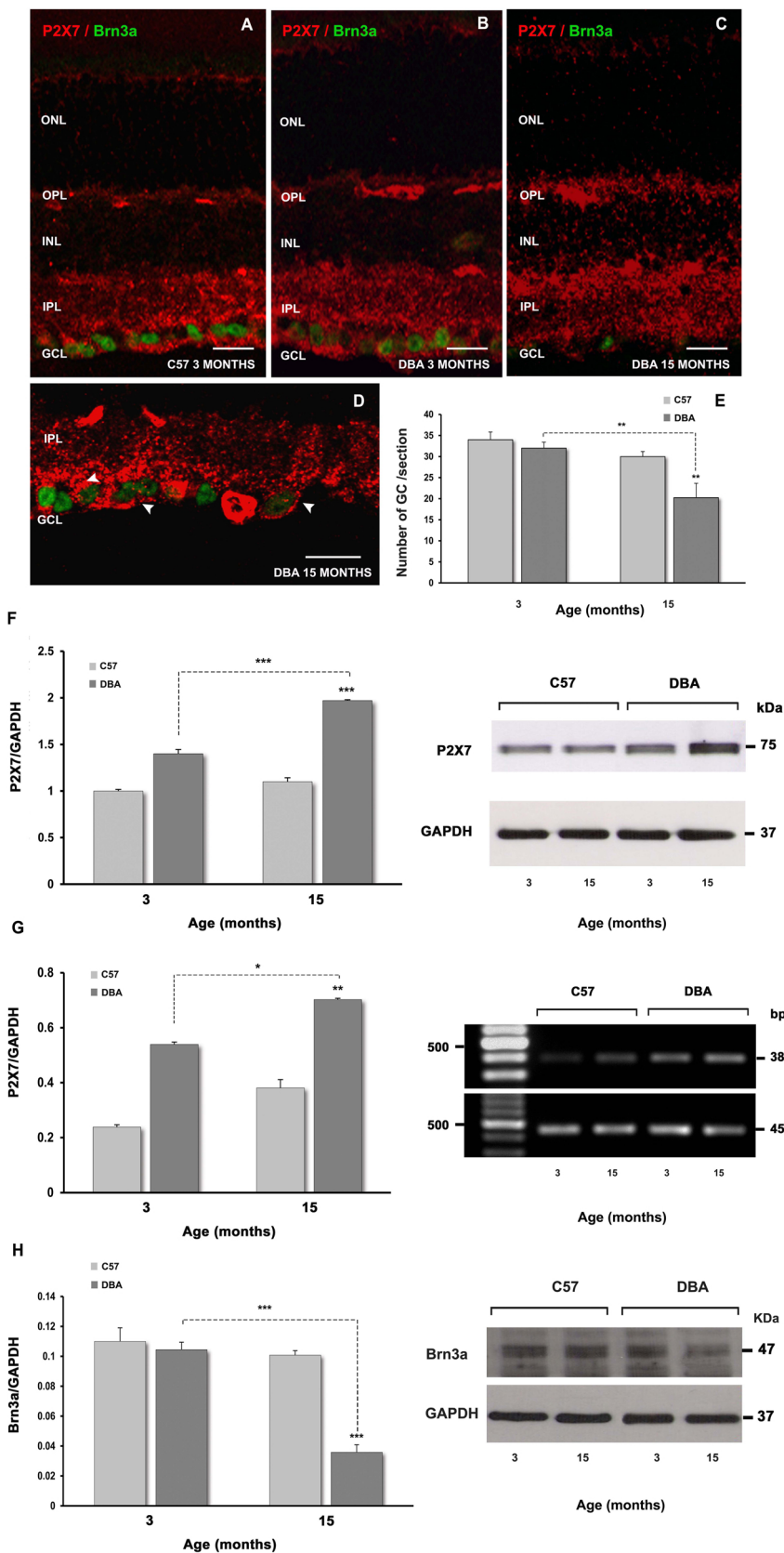


Fig. 2. Up-regulated P2X7 receptor and Brn3a decrease during the development of the pathology (from 3 to 15 months) in DBA/2J and control mice retina. (A–D) P2X7 and Brn3a immunostaining in mice retinas. P2X7 immunoreactivity in retinal ganglion cells (and retinal inner layers) during the development of glaucoma. P2X7R were increased in DBA/2J retina from 3 to 15 months of age (B, C and D). In normal retinas (C57BL/6J and DBA/2J at 3 months), Brn3a immunoreactivity was observed in RGCs. However, when the retinal impairment progresses Brn3a immunoreactivity was observed in a smaller population of Brn3a, and this correlates with RGC loss. (D) High magnification from DBA/2J retina at 15 months shows the strong P2X7 immunoreactivity in RGCs. All images were acquired at 20x magnification. Merge. Scale bars: 20 μ m. (E) Quantification of the number of RGCs in vertical sections labelled with Brn3a in control (C57) and glaucomatous (DBA) mice at 3 and 15 months of age and expressed as mean \pm SEM. Student's *t*-test (**p* < 0.05; ***p* < 0.01; ****p* < 0.001). (F) Western blot on retinal extracts at 3 and 15 months in C57BL/6J and DBA/2J mice, showing an increased expression of P2X7R in pathological mice. GAPDH were used as a control to normalize P2X7 levels. Data were represented as mean \pm SEM. Student's *t*-test (****p* < 0.001). (G) RT-PCR was done using primers as described in material and methods. GAPDH was used as an internal control. The values of the ratio of P2X7 to GAPDH were calculated and data were normalized by threshold recordings in control and glaucomatous mice at 3 and 15 months. mRNA levels of the control, defined as 100% (**p* < 0.05; ***p* < 0.01). (H) Western blot analysis of the Brn3a expression showed a significant decrease between 3 and 15 months in DBA/2J mice, GAPDH were used as a control to normalize Brn3a levels. Data were represented as mean \pm SEM. Student's *t*-test (****p* < 0.001).

3.3. Morphological alterations in glaucoma model

Immunohistochemistry studies were carried out to identify morphological alterations in DBA/2J glaucomatous mice. Specific retinal

markers were evaluated in the progression of disease and their possible relationship with P2X7R. The results reveal significant changes including a loss of synaptic vesicles, the presence of retinal gliosis, RGC death and abnormal expression of RGC neurofilaments associated with

neurodegeneration or neuronal damage.

3.3.1. Retinal ganglion cell loss

The expression of Brn3a was observed in the GCL of control and pathological retinas (Fig. 2 A–C). At 15 months, when the retinal dysfunction was detected, Brn3a immunoreactivity had decreased due to RGC loss. The quantification of Brn3a expression by western blot showed a reduction of 64.3% ($p < 0.0005$) (Fig. 2H). In addition, when the number of RGCs in control and injured sections were counted to correlate the reduction in protein levels (Fig. 2E) a decrease of 36.71% $p < 0.005$ was observed. Double labeling with the neuronal marker Brn3a revealed that the majority of RGCs were showing a positive P2X7 immunostaining (Fig. 2D). A significant P2X7R immunostaining increase was found in the small population of surviving RGCs (Fig. 2D). These results suggest the possible contribution to P2X7R-mediated RGC neurodegeneration.

3.3.2. Reactive gliosis in glaucomatous mice

GFAP, extensively used as a marker for reactive gliosis, was analyzed by western blot in glaucomatous and control mice at different ages (3 or 15 months). In older DBA/2J mice retinas, GFAP was increased 3.74 fold (374% of increase) in glial cells in response to neuronal damage comparing with control mice ($p < 0.01$). The GFAP levels were increased with aging in glaucomatous mice 1.84 (84% of increase) fold ($p < 0.01$) in contrast with DBA/2J 3 months old (Fig. 3 D–E). Immunohistochemical results (Fig. 3) indicate that when compared to control mice, GFAP-immunoreactivity was increased in astrocytes and Müller cells in a time-dependent manner (Fig. 3 A–C) in DBA/2J mice.

3.3.3. Loss of synaptic connectivity

In order to clarify the possible alteration in retinal circuitry, the connectivity between photoreceptors and second order retinal neurons was studied using synaptophysin (SYP) marker. The P2X7 and SYP expression were analyzed to establish their possible contribution with the concomitant inner retinal damage. In 15 months old DBA/2J retinas (Fig. 4C) a different pattern of expression of the SYP synaptic vesicle protein with respect to DBA/2J mice at 3 months old was detected. In the DBA/2J mice, it is observed a reduction of the photoreceptor axon terminals. The levels of Syp were analyzed by western blot technique. There was a 30.36% reduction in DBA/2J mice of 15 months of age when compared to younger mice ($p < 0.05$). However, in C57BL/6J mice there were no significant changes detected with age (Fig. 4D). Glaucomatous degeneration may cause synapse alteration. The SYP is an integral membrane protein of the synaptic vesicles involved in multiple functions as exocytosis, neurotransmitter delivery and retinal development. Double immunolabeling experiments with P2X7 and SYP could reveal the axon photoreceptor terminal damaged and this may lead to apoptotic processes in second order neurons.

3.3.4. Neurofilaments

In whole-mounted retinas we have studied qualitatively the expression of pNFH and P2X7 receptor, a well-established degeneration marker of RGC lesion, according to its abnormal cellular distribution pattern, and a mediator in neuronal death, respectively; at two ages, 3 and 15 months (Fig. 5).

At early stages (3 months old) the qualitative study of P2X7 and pNFH co-expression on whole-mount retinas revealed no morphological signs of neuronal degeneration in the RGC population of DBA/2J mouse at this age (Fig. 5A', A'', B', B'', C', C''). Its appearance was like that observed in control retinas (C57BL/6J mice) at the same age (Fig. 5A, B, C). At this age, pNFH positive RGC (pNFH⁺ RGC) immunoreactivity shows the typical expression pattern described in healthy neurons by other authors (Parrilla-Reverter et al., 2009) (Fig. 5A-A''). In the intraretinal aspect of the RGC, the expression of pNFH appears restricted mainly to the distal portion of the axons, where axons are tightly

packed in bundles arranged radially in the central region of the retina around the optic disk. There were no signs of pNFH up-regulation in the RGC soma, proximal axon or dendrites. In the peripheral and middle retina, there was no pNFH positive immunoreactivity or it was scarce and sparse, like in control retinas. The expression of the P2X7 receptor was absent in the RGC population, only it was observed as slight P2X7 positive immunoreactivity in the innermost vascular plexus of the retina of both control (C57BL/6J) (Fig. 5B, C) and DBA/2J (Fig. 5 B', B'', C', C'') mice at 3 months of age. These morphological data about expression of both neurodegeneration markers were consistent with functional data observed in these animals, where there was no sign of abnormal function in the retina (Fig. 1).

At 15 months of age (Fig. 5 D-D'', E-E'', F-F'') immunodetection of both markers (pNFH and P2X7) on whole-mounted retinas made easy correlate the observed neuronal degeneration in our results with the typical and characteristic patched pattern of neuronal degeneration in the retina of DBA/2J mice (Fig. 5D', D'', E', E''). This mouse lineage is characterized by a large inter- and intra-individual variability during the development of the pathological condition along the time. It was possible to observe old mice without retinal pathological signs or, even, animals that only developed a total or partial lesion in one of both retinas. Degeneration pattern was revealed by diminution in the density of axonal bundles in the central retina and abnormal pNFH positive immunoreactivity in the RGC soma and proximal axon. These RGCs were scattered throughout the retina, without a clear regionalization, alternating with typical pNFH immunopositive axons from healthy RGC. Axons and nerve fiber bundles lose their straight trajectory and those observed showed a wavy line path characteristic of the axons from RGCs in degeneration (Fig 5D', D''). The expression of P2X7 was mainly restricted to the cell body of pNFH⁺ RGC in animals with severely damaged retinas or those where the degeneration was not so obvious (Fig. 5E', E'', F', F''). P2X7 was not immunodetected in RGC from control animals (Fig. 5E, F). However, it was striking the down-regulation of the expression of P2X7R in the vascular system of the DBA/2J mice at 15 months of age, because this downregulation was not observed in control mice of the same age neither in DBA/2J mice at 3 months of age and its controls (Fig. 5E-E'', F-F''). This loss of vascular immunostaining was observed in retinas with clear signs of degeneration and in those in which the glaucomatous condition was not detected on the base of an aberrant pNFH expression in RGC.

3.4. Activation of p38, JNK and apoptotic processes mediated by caspase-3 in retinal ganglion cells

3.4.1. P38 and JNK phosphorylation

The possible implication of MAPKs was evaluated during the apoptotic process induced by the development of glaucomatous degeneration (Fig. 6A, B). The activation of two members of the MAPK family, JNK54/46 (Fig. 6A) and p38 (Fig. 6B), was monitored by western blot analysis with antibodies that recognize the activated phosphorylated forms of the two kinases.

Retinal protein lysates were analyzed at different ages comparing the evolution of the pathology and with control mice. The expression levels of phospho-JNK54/46 were up-regulated in injured retinas finding 79.35% of increase, when comparing with the control mice at 15 months. A statistically significant increase of 55.10% $p < 0.005$ was observed in DBA/2J mice with age (Fig. 6A). In addition to JNK, the expression levels of phosphorylated p38 protein (Fig. 6B) were higher at 15 months than at 3 months in the DBA/2J mice (an increase of 342%), when compared with control mice at 15 months ($p < 0.001$, Fig. 6B). Non-significant age-dependent decrease was observed in the phosphorylated proteins levels obtained at 3 or 15 month old C57BL/6J mice. The total MAPK protein level p38 and JNK54/56 levels remained constant over the time course (Fig. 6A, B right panels).

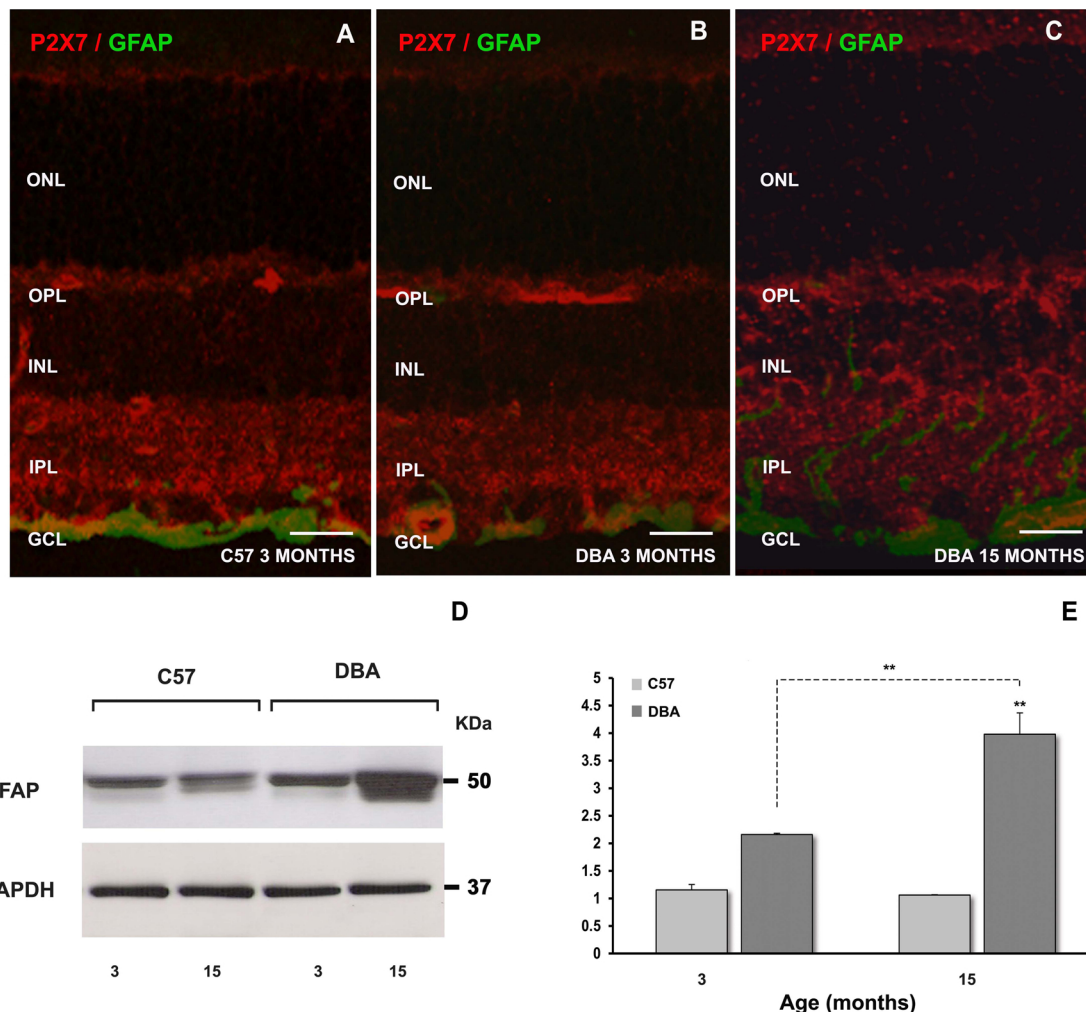


Fig. 3. Glial cells are activated in glaucomatous retinas. (A–C) Glial cell activation was assessed by immunostaining retinal cross sections with antibodies against GFAP (green) in C57BL/6J (A) and DBA/2J retinas (B–C). In the C57 and 3 months old DBA retinas, GFAP immunoreactivity was selectively localized to astrocytes (in mouse retina there is no detectable GFAP in Müller cell endfeet). In 15 months old DBA/2J mice, GFAP reactivity of Müller cells extended from the inner to the outer retina. On merged images, P2X7R was found to co-localize strongly with GFAP in the retina of glaucomatous mice. All images were acquired at 20x magnification. Merge. Scale bars: 20 μ m. (D) Western blot analysis of the GFAP levels in control and glaucomatous retina at 3 and 15 months. Membrane was probed with anti-GAPDH antibody as a loading control. Student's *t*-test (** $p < 0.01$).

3.4.2. Caspase-3 activation

In previous studies, we characterized the loss of RGC in this murine glaucoma model (Pérez de Lara et al., 2014). Therefore, to evaluate the cell death produced by apoptosis we analyzed the expression of caspase-3. Western blot analysis of retinal protein extracts showed weakly expression in non-pathological retinas (control retinas and younger DBA/2J retinas) but during the development of the pathology its expression increased significantly (279.82% $p < 0.001$) when compared to C57BL/6J control matched mice (Fig. 6C).

Immunoblot results were correlated with caspase-3 activity. Lysate retinal extracts were collected from control and DBA/2J mice at 3 and 15 months. A large increase in Ac-DEVD-N³-MC-R110 cleavage was observed in glaucomatous retinas. As shown, in Fig. 6, caspase-3 activity was statistically increased at 15 months of age in DBA/2J mice (288%, $p < 0.001$) compared with wild type retinas at 3 or 15 months and DBA/2J retinas at 3 months (Fig. 6D).

4. Discussion

In the present study, we assess the increased expression of the ATP-gated P2X7R in the retina of DBA/2J glaucomatous mice during the development of the pathology. This increase can be correlated with

specific retinal markers. GFAP, SYP, NF and Brn3a expression change in this animal model as the pathology advances. Furthermore, the present work describes the possible role of P2X7 nucleotide receptor on p-p38 and p-JNK activation and their possible implication with RGC apoptotic death through caspase-3 pathway.

4.1. Loss of RGC in DBA mice and retinal dysfunction

DBA/2J mouse is a well-established model of glaucoma characterized by a progressive loss of RGCs and optic nerve excavation (Nagaraju et al., 2007; Buckingham et al., 2008; McKinnon et al., 2009). In this pigmented glaucoma mice model, the possible mechanisms of RGC death were investigated. A qualitative and quantitative reduction of Brn3a expression during the progress of the pathology in DBA/2J mice were detected. In Brn3a immunodetected DBA/2J retina cross-sections, the number of RGCs significantly decreased with age, in accordance with previous studies (Fernandez-Sanchez et al., 2014). Our results are according to previous findings (Pérez de Lara et al., 2014) and the degeneration in retinal patches described by Fernandez-Sanchez and co-workers (Fernandez-Sanchez et al., 2014). These values were confirmed with the down-regulated protein levels detected by western blot (Fig. 2). RGCs loss in this model is a consequence of iris pigment

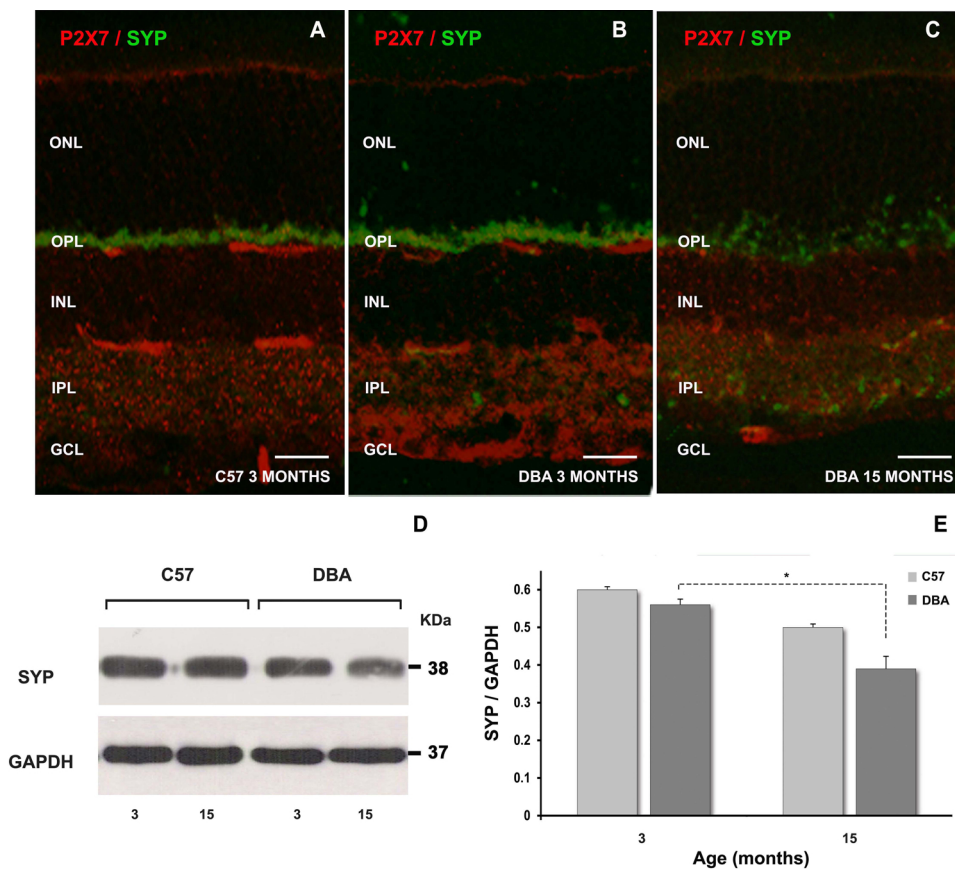


Fig. 4. Immunolabeling of synaptophysin (green) and P2X7R (red) in control and glaucomatous retinas at different ages (3 and 15 months) (A–C). At 15 months (C), SYP immunostain shows a dissipation and clustering pattern of the label in the OPL and a more prominent clustering in the SYP label in the IPL than at 3 months (B) and control (A). All images were acquired at 20x magnification and merge. Scale bars: 20 μ m. Western blot analysis of the SYP levels in control and glaucomatous retina at 3 and 15 months (D). The amount of SYP decreased significantly during the progress of the pathology (E). Membrane was probed with anti-GAPDH antibody as a loading control. Student's *t*-test (**p* < 0.05).

dispersion (IPD) and iris stromal atrophy (ISA) (John et al., 1998; Saleh et al., 2007). Because of the ISA and IPD mutation are involved in defects in melanin synthesis promoting cytotoxicity. The detached pigments insult the ocular drainage structures and IOP increase concomitantly (Anderson et al., 2002, 2006). Based on these findings, DBA/2J RGCs degenerate accompanied by the reduction of the scotopic threshold response (STR) at 15 months which indicates a loss of RGC function.

4.2. P2X7 receptor and the glaucoma pathogenesis

Different models of neurodegeneration associate P2X7 receptors as a candidate involved in the pathogenesis of neurodegenerative disorders (Diaz-Hernandez et al., 2009, 2012; Jimenez-Pacheco et al., 2013). Altered extracellular ATP concentrations and activation of P2X7 may contribute to the pathologic loss of RGC and retinal dysfunction (Resta et al., 2005; Reigada et al., 2008; Puthussery and Fletcher, 2009; Hu et al., 2010; Sugiyama et al., 2010; Niyadurupola et al., 2013). Furthermore, previous *in vitro* studies have demonstrated the involvement of ATP in induced neuronal apoptosis through P2X7 receptor. In fact, stimulation of P2X7 receptor with Benzoyl-ATP induced apoptosis in cultured RGC of rat (Zhang et al., 2005) and hypoxia or higher ocular pressure-induced RGC death were mediated by P2X7 receptor (Reigada et al., 2008; Mitchell et al., 2009; Sugiyama et al., 2010). In the present study we observed up-regulation of P2X7R in glaucomatous mice at 15 months. Increasing P2X7 receptor levels was more remarkable in the inner retina (GCL and IPL), in accordance with progressive morphological alterations. P2X7R stimulation may induce RGC apoptosis in advanced stages, and thus abolish Brn3a transcription factor expression. This would be consistent with evidence from isolated rat RGCs where P2X7R stimulation led to calcium overload, caspase activation and subsequent apoptosis (Zhang et al., 2005). The significant RGC loss was evident by a significant diminution in axonal density as the pathology

progresses when RGCs were reduced and the abnormal pNFH positive immunoreactivity was present, using this protein as axonal marker (Fig. 5). Moreover, this finding correlates with morphological alterations and molecular changes in the DBA/2J mice.

P2X7R expression has been detected in mice astrocytes in a glaucomatous model (Vessey and Fletcher, 2012). In the present work an increase in GFAP expression at the age of glaucoma onset has been detected. Astrocytes labeled with GFAP were found to co-localize with P2X7R in the mouse retina, as carefully described by Vessey and Fletcher (Vessey and Fletcher, 2012). The P2X7R presence suggests the implication of this receptor in regulating microglial activity (Monif et al., 2010). The presence of activated P2X7R may be involved with inflammatory responses in inner retina as described *in vitro* (Panenka et al., 2001). In addition, an increase of P2X7R was observed in OPL accompanied by a diminished synaptic connectivity in older animals. Increased levels of P2X7R were detected in synaptic terminal suggesting the possible apoptotic processes involved due to the impairment of retinal circuitry (Puthussery et al., 2006; Heiduschka et al., 2010). This result is in agreement with previous morphological findings where a loss of synaptic contacts in the OPL in an aging-dependent manner was observed in this model (Fernandez-Sanchez et al., 2014). This may suggest the implication of P2X7 in photoreceptor pathway signaling and other indirect mechanisms that could contribute to P2X7R-mediated RGC neurodegeneration (Puthussery et al., 2006; Vessey and Fletcher, 2012). Moreover, increased extracellular ATP levels at advanced stages contribute to P2X7R activation and could be implicated in retinal microvasculature damage. Several reports suggest that P2X7 activation triggers cell death in inflammatory retinal diseases (Sugiyama et al., 2004, 2005). It is tempting to suggest that upregulation of this receptor may mediate apoptosis in the retinal microvasculature and epithelial cells could be suffering morphological re-structuring and integrity loss as the pathology progresses in aged (15 months old) glaucomatous mice.

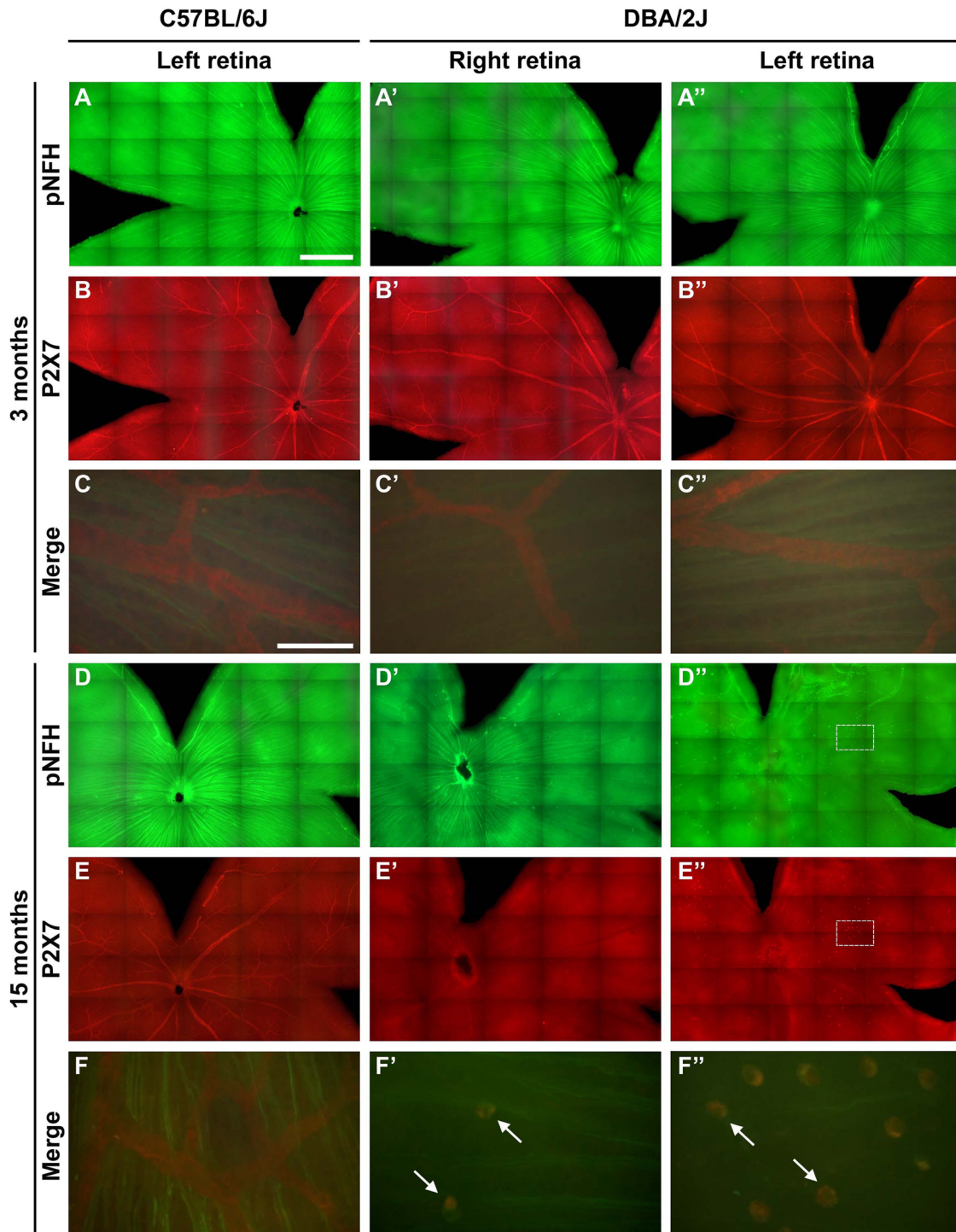


Fig. 5. Retinal ganglion cell axonal pattern in control and glaucomatous mice (A–F). Representative illustrations from whole-mount retinas of control (C57BL/6J) and DBA/2J mice at 3 and 15 months of age are shown. At 3 months old, in control (A, C) and DBA/2J (A', A'', C', C'') mice intense pNFH-expression is detected in bundles of RGC axons radially converging towards the optic disk within the central area of the retina. Note that in control and 3 months old DBA/2J retinas pNFH-expression do not reach the periphery of the retina nor is observed in the cell bodies or dendrites of RGCs. P2X7R-expression is null in the RGC population in control (B, C, E, F) and in 3 months old DBA/2J (B', B'', C', C'') retinas. Notice that retinal innermost vascular plexus shows P2X7R positive immunoreaction at 3 months (B–B''). There is no co-expression of both markers at 3 months stage (C–C''). At 15 months of age comparing with control retinas (D), there are changes of the pNFH-expression pattern in DBA/2J retinas (D', D''). The number of immunopositive RGC axons diminishes in the center of the retina and RGC somas with abnormal pNFH-expression appear scattered throughout the retina (D', F') or decrease dramatically throughout the retina and the abnormal pNFH-expression is restricted to the RGC somas (D'', F''). Note the strong variability in the degree of retinal degeneration in DBA/2J mice retinas (D'', F''). Comparing with control (E, F), P2X7R-expression appear restricted to RGC somas (E', E'') in co-expression with pNFH (F', F''); arrows) in degenerated retinas. There is no vascular plexus P2X7R labeling in neurodegenerated retinas (E', E''), in contrast with that observed in control (E). Detail of square region in D'' and E'' is showed in F'' to show the double labeling of the RGC somas in retinas with severe neurodegeneration. Scale bar 500 μm (A–A'', B–B'', D–D'', E–E''). Scale bar 50 μm (C–C'', F–F'').

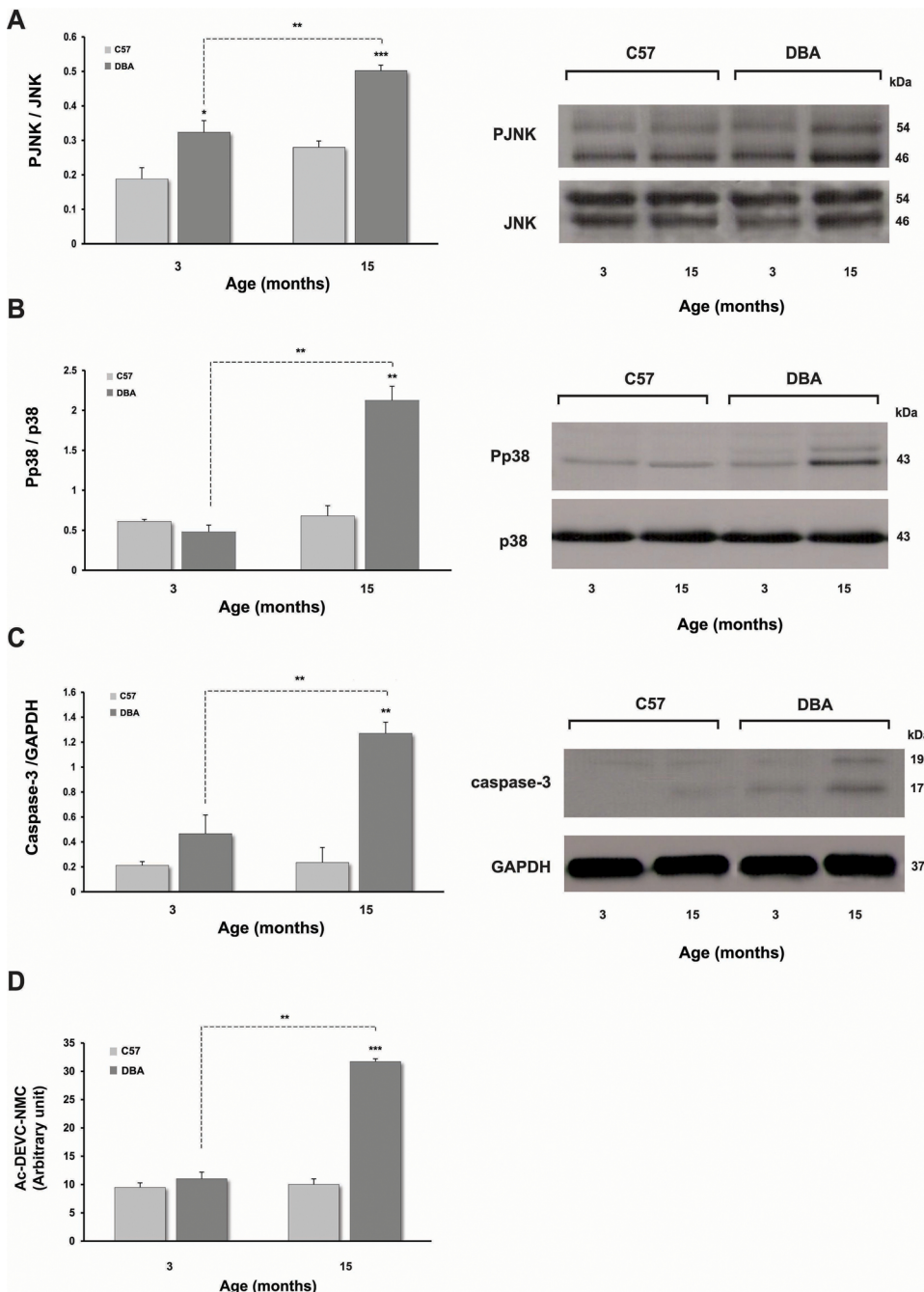


Fig. 6. Western blot time-course analysis of JNK, p38 and caspase-3 (A–C) and retinal activity of caspase-3 (D) in the glaucomatous and control retinas. JNK, p38 and caspase-3 are overexpressed in glaucomatous retinas. (A–C) Densitometry analysis showed that at 15 months, there was a significant increase in JNK (A), p38 (B) and caspase-3 (C) when compared with the control and 3 months old glaucomatous DBA/2J retinas. p-MAPKs (JNK and p38) were not significantly affected with age in control mice. GAPDH was used as a loading control. Values represent mean \pm SD (n = 10) (*p < 0.05; **p < 0.01; ***p < 0.001). (D) Caspase-3 activation was measured by incubating control and glaucomatous mice retinas with a fluorescent caspase-3 substrate, as described in Material and Methods. The enzyme activity was significantly increased in the DBA/2J retinas at 15 months compared with the control and younger glaucomatous mice. Data are presented as mean \pm SD (n = 4) (**p < 0.01; ***p < 0.001).

4.3. Involvement of p38 and JNK MAP kinases in glaucomatous degeneration

The P2X7 receptor has been associated with multiple signaling cascades, resulting in activation of phospholipase D, cytokine release, cytoskeletal rearrangements and MAPKs (Skaper et al., 2010). Several studies have shown that activation of P2X7 receptor leads to downstream activation of p38 (Ono and Han, 2000; Armstrong et al., 2002; Donnelly-Roberts et al., 2004) and JNK MAPKs (Suzuki et al., 2004). The cell death of GCL and INL neurons in glaucoma is known to involve the activation of JNK and p38 intracellular pathways (Kikuchi et al., 2000; Levkovitch-Verbin et al., 2005; Munemasa et al., 2005, 2006; Bessero et al., 2010; Donovan et al., 2011). Increased JNK and p38 MAPK signaling has also been documented in human glaucomatous tissue (Tezel et al., 2003). Moreover, it was reported that inhibition of

JNK and p38 protects neurons from retinal NMDA-induced neurotoxicity (Munemasa et al., 2005). Considering this, recent studies suggest a protective role of P2X7 receptor antagonists (Di Virgilio et al., 2001; Franke et al., 2004; Jun et al., 2007; Diaz-Hernandez et al., 2009; Chen et al., 2013). In the present study we have detected alterations in the expression of several proteins related to RGC death in the retina of DBA/2J mice. Our data showed an activation of the phospho-MAPK family members JNK and p38 in injured retinas compared with the control mice at 15 months (Fig. 6). The findings obtained from the western blot analysis showed different expression profiles of the MAPK members, suggesting different roles of JNK and p38 proteins in P2X7-induced retinal changes. Our results showed the activation of MAPK signaling in injured up-regulated P2X7R retinas. Overall, these findings suggest that JNK and p38 pathways, are pro-apoptotic in P2X7 induced ganglion cells death.

4.4. Activation of apoptotic pathways/mechanisms

Neuronal apoptosis induced by P2X7R activation requires ATP released from excited or damaged cells as consequence of ocular injury. Extracellular ATP increased levels may be linked to the activation of the P2X7R in glaucomatous injury (Resta et al., 2007; Reigada et al., 2008). Recent research shows increased extracellular ATP levels in the DBA/2J model (Perez de Lara et al., 2015, 2018), which, together with the P2X7 increased receptor expression described in this work, suggests that its activation may trigger the subsequent underlying intracellular cascades already described. In this sense, many studies have demonstrated that the activation of the caspase cascades in neuronal cells plays an important role in programmed RGC death (Morrison et al., 1997; Sawada and Neufeld, 1999; Kim and Park, 2005; Zhang et al., 2005; Reichstein et al., 2007; Sugiyama et al., 2013). Caspase-mediated cell death is regulated in part by MAP kinase cascades. JNK is known to be involved in axonal injury signaling and apoptosis (Donovan et al., 2011; Fernandes et al., 2012; Harder et al., 2012). Several up-regulated proteins have been documented in a model of optic nerve transection regulating apoptotic pathways (Agudo et al., 2009). Similarly, p38 MAPK activation has been implicated as an upstream of caspase mediator developing RGC injury in different experimental models of glaucoma, including optic nerve axotomy, ocular hypertension, and excitotoxic injury (Kikuchi et al., 2000; Manabe and Lipton, 2003; Harada et al., 2006; Levkovitch-Verbin et al., 2007; El-Remessy et al., 2008). Furthermore, recent reports describe the inhibition of p38 as a therapeutic target in filtering glaucoma surgery in rabbits (Nassar et al., 2015) and axonal dysfunction models (Dapper et al., 2013). The distribution of these stress activated proteins in the mouse retina includes INL and GCL and its expression levels have been found by proteomic analysis increased in retinal neurotoxicity (Munemasa et al., 2005; Bessero et al., 2010), glaucomatous damage (Dapper et al., 2013) and retinal ischemia (Roth et al., 2003).

All these reports are consistent with the present results describing the possible connection between stress-activated proteins (p38, JNK) and caspases (Chen et al., 2013; Dapper et al., 2013). We have demonstrated that these proteins expression was significantly increased with age in DBA/2J retinas together with the concomitant apoptotic RGC death. It was also observed the subsequent caspase-3 activation through upstream regulation during the progress of glaucomatous degeneration. We have investigated the protein levels and activity of caspase-3 in retinal tissue from controls and glaucoma animals. In this sense, a significantly increased activity of caspase-3 at 15 months correlated with the observed increased level of the active p20 fragment of up-regulated protein (Fig. 6).

In this study, the possible involvement of caspase-3 in P2X7 receptor-induced pathway of MAPK (JNK and p38) activation has been suggested. The results indicate that a sustained concentration of extracellular ATP may activate caspase-3 pathway playing a role in coupling the P2X7 receptor to the MAPK signaling cascade. Therefore, the antagonism of P2X7R may be a possible approach to prevent ganglion cell death in glaucoma pathogenesis. The inhibition of P2X7R has been previously reported in different models of neurodegenerative diseases. *In vivo* administration of a P2X7R antagonist, demonstrated significant reductions in amyloid plaques in Alzheimer disease model via glycogen synthase kinase-3 (Diaz-Hernandez et al., 2012) and prevent neuronal apoptosis and induced brain damage in Huntington's disease and epilepsy (Diaz-Hernandez et al., 2009; Jimenez-Pacheco et al., 2013). Similar findings were described in an induced IOP elevation rat model (Sugiyama et al., 2013), and in *in vivo* stimulation of P2X7R (Hu et al., 2010).

4.5. Conclusions

In summary, we have described the P2X7R, GFAP, SYP, NF expression and the apoptotic signaling components altered in a mouse

model of human pigmentary glaucoma. These findings indicate that events of synaptic loss, GFAP activation, NF deficit and apoptosis could be involved in the pathogenesis of glaucoma leading to visual dysfunction. Identifying the molecular mechanisms and intracellular pathways activated to promote cell dysfunction and concomitant neuronal death in this glaucomatous model will provide a basis for developing and targeting treatments for retinal neurodegenerative diseases.

This study provides evidences of molecular alterations in the retina associated with glaucomatous damage. MAPK signaling pathways may be involved in P2X7 activation mediated pathogenesis of pigmentary glaucoma in DBA/2J retinas. Altered protein levels were found to be related with impairment of inner retina led by apoptotic cascades. Further studies are necessary to elucidate the role of P2X7 and the implicated mechanisms underlying RGC injury.

Acknowledgments

This article is dedicated to Prof. Jesús Pintor, who died at the time this manuscript was under revision.

This work was supported by research grants from the Spanish Ministry of Economy and Competitiveness, Fondo Europeo de Desarrollo Regional “una manera de hacer Europa” (SAF-2013-44416-R, SAF-2016-77084-R, and SAF-2015-67643-P), the Spanish Ministry of Health Social Services and Equality (RETICS RD16/0008/0017, RD16/0008/0020, RD16/0008/0026, and RD12/0034/0001) and Fundación Séneca, Agencia de Ciencia y Tecnología de la Región de Murcia, Spain (19881/GERM/15).

Appendix A. Supplementary data

Supplementary material related to this article can be found, in the online version, at doi:<https://doi.org/10.1016/j.brainresbull.2019.05.006>.

References

- Adinolfi, E., Kim, M., Young, M.T., Di Virgilio, F., Surprenant, A., 2003. Tyrosine phosphorylation of HSP90 within the P2X7 receptor complex negatively regulates P2X7 receptors. *J. Biol. Chem.* 278, 37344–37351.
- Aga, M., Watters, J.J., Pfeiffer, Z.A., Wiep, G.J., Sommer, J.A., Bertics, P.J., 2004. Evidence for nucleotide receptor modulation of cross talk between MAP kinase and NF-kappa B signaling pathways in murine RAW 264.7 macrophages. *Am. J. Physiol., Cell Physiol.* 286, C923–930.
- Agudo, M., Perez-Marin, M.C., Lonngren, U., Sobrado, P., Conesa, A., Canovas, I., Salinas-Navarro, M., Miralles-Imperial, J., Hallbook, F., Vidal-Sanz, M., 2008. Time course profiling of the retinal transcriptome after optic nerve transection and optic nerve crush. *Mol. Vis.* 14, 1050–1063.
- Agudo, M., Perez-Marin, M.C., Sobrado-Calvo, P., Lonngren, U., Salinas-Navarro, M., Canovas, I., Nadal-Nicolas, F.M., Miralles-Imperial, J., Hallbook, F., Vidal-Sanz, M., 2009. Immediate upregulation of proteins belonging to different branches of the apoptotic cascade in the retina after optic nerve transection and optic nerve crush. *Invest. Ophthalmol. Vis. Sci.* 50, 424–431.
- Alarcon-Martinez, L., de la Villa, P., Aviles-Trigueros, M., Blanco, R., Villegas-Perez, M.P., Vidal-Sanz, M., 2009. Short and long term axotomy-induced ERG changes in albino and pigmented rats. *Mol. Vis.* 15, 2373–2383.
- Anderson, M.G., Smith, R.S., Hawes, N.L., Zabaleta, A., Chang, B., Wiggs, J.L., John, S.W., 2002. Mutations in genes encoding melanosomal proteins cause pigmentary glaucoma in DBA/2J mice. *Nat. Genet.* 30, 81–85.
- Anderson, M.G., Libby, R.T., Mao, M., Cosma, I.M., Wilson, L.A., Smith, R.S., John, S.W., 2006. Genetic context determines susceptibility to intraocular pressure elevation in a mouse pigmentary glaucoma. *BMC Biol.* 4, 20.
- Armstrong, J.N., Brust, T.B., Lewis, R.G., MacVicar, B.A., 2002. Activation of presynaptic P2X7-like receptors depresses mossy fiber-CA3 synaptic transmission through p38 mitogen-activated protein kinase. *J. Neurosci.* 22, 5938–5945.
- Barhoun, R., Martinez-Navarrete, G., Corrochano, S., Germain, F., Fernandez-Sanchez, L., de la Rosa, E.J., de la Villa, P., Cuenca, N., 2008. Functional and structural modifications during retinal degeneration in the rd10 mouse. *Neuroscience* 155, 698–713.
- Bessero, A.C., Chiodini, F., Rungger-Brandle, E., Bonny, C., Clarke, P.G., 2010. Role of the c-Jun N-terminal kinase pathway in retinal excitotoxicity, and neuroprotection by its inhibition. *J. Neurochem.* 113, 1307–1318.
- Buckingham, B.P., Inman, D.M., Lambert, W., Oglesby, E., Calkins, D.J., Steele, M.R., Vetter, M.L., Marsh-Armstrong, N., Horner, P.J., 2008. Progressive ganglion cell degeneration precedes neuronal loss in a mouse model of glaucoma. *J. Neurosci.* 28, 2735–2744.
- Casson, R.J., 2006. Possible role of excitotoxicity in the pathogenesis of glaucoma. *Clin.*

- Experiment. Ophthalmol. 34, 54–63.
- Catanzaro, J.M., Hueston, C.M., Deak, M.M., Deak, T., 2014. The impact of the P2X7 receptor antagonist A-804598 on neuroimmune and behavioral consequences of stress. *Behav. Pharmacol.* 25, 582–598.
- Chen, S., Ma, Q., Krafft, P.R., Chen, Y., Tang, J., Zhang, J., Zhang, J.H., 2013. P2X7 receptor antagonism inhibits p38 mitogen-activated protein kinase activation and ameliorates neuronal apoptosis after subarachnoid hemorrhage in rats. *Crit. Care Med.* 41, e466–474.
- Cuenca, N., Pinilla, I., Fernandez-Sanchez, L., Salinas-Navarro, M., Alarcon-Martinez, L., Aviles-Trigueros, M., de la Villa, P., Miralles de Imperial, J., Villegas-Perez, M.P., Vidal-Sanz, M., 2010. Changes in the inner and outer retinal layers after acute increase of the intraocular pressure in adult albino Swiss mice. *Exp. Eye Res.* 91, 273–285.
- Dapper, J.D., Crish, S.D., Pang, I.H., Calkins, D.J., 2013. Proximal inhibition of p38 MAPK stress signaling prevents distal axonopathy. *Neurobiol. Dis.* 59, 26–37.
- Di Virgilio, F., Chiozzi, P., Falzoni, S., Ferrari, D., Sanz, J.M., Venketaraman, V., Baricordi, O.R., 1998. Cytolytic P2X purinoceptors. *Cell Death Differ.* 5, 191–199.
- Di Virgilio, F., Chiozzi, P., Ferrari, D., Falzoni, S., Sanz, J.M., Morelli, A., Torboli, M., Bolognesi, G., Baricordi, O.R., 2001. Nucleotide receptors: an emerging family of regulatory molecules in blood cells. *Blood* 97, 587–600.
- Diaz-Hernandez, M., Diez-Zaera, M., Sanchez-Nogueiro, J., Gomez-Villafuertes, R., Canals, J.M., Alberch, J., Miras-Portugal, M.T., Lucas, J.J., 2009. Altered P2X7-receptor level and function in mouse models of Huntington's disease and therapeutic efficacy of antagonist administration. *FASEB J.* 23, 1893–1906.
- Diaz-Hernandez, J.I., Gomez-Villafuertes, R., Leon-Otegui, M., Hontecillas-Prieto, L., Del Puerto, A., Trejo, J.L., Lucas, J.J., Garrido, J.J., Gualifa, J., Miras-Portugal, M.T., Diaz-Hernandez, M., 2012. In vivo P2X7 inhibition reduces amyloid plaques in Alzheimer's disease through GSK3beta and secretases. *Neurobiol. Aging* 33, 1816–1828.
- Donnelly-Roberts, D.L., Namovic, M.T., Faltynek, C.R., Jarvis, M.F., 2004. Mitogen-activated protein kinase and caspase signaling pathways are required for P2X7 receptor (P2X7R)-induced pore formation in human THP-1 cells. *J. Pharmacol. Exp. Ther.* 308, 1053–1061.
- Donovan, M., Doonan, F., Cotter, T.G., 2011. Differential roles of ERK1/2 and JNK in retinal development and degeneration. *J. Neurochem.* 116, 33–42.
- El-Remessy, A.B., Tang, Y., Zhu, G., Matragoon, S., Khalifa, Y., Liu, E.K., Liu, J.Y., Hanson, E., Mian, S., Fatteh, N., Liou, G.I., 2008. Neuroprotective effects of cannabidiol in endotoxin-induced uveitis: critical role of p38 MAPK activation. *Mol. Vis.* 14, 2190–2203.
- Fernandes, K.A., Harder, J.M., Fornarola, L.B., Freeman, R.S., Clark, A.F., Pang, I.H., John, S.W., Libby, R.T., 2012. JNK2 and JNK3 are major regulators of axonal injury-induced retinal ganglion cell death. *Neurobiol. Dis.* 46, 393–401.
- Fernandez-Sanchez, L., de Sevilla Muller, L.P., Brecha, N.C., Cuenca, N., 2014. Loss of outer retinal neurons and circuitry alterations in the DBA/2J mouse. *Invest. Ophthalmol. Vis. Sci.* 55, 6059–6072.
- Franke, H., Gunther, A., Grosche, J., Schmidt, R., Rossner, S., Reinhardt, R., Faber-Zuschratter, H., Schneider, D., Illes, P., 2004. P2X7 receptor expression after ischemia in the cerebral cortex of rats. *J. Neuropathol. Exp. Neurol.* 63, 686–699.
- Franke, H., Klimke, K., Brinckmann, U., Grosche, J., Francke, M., Sperlagh, B., Reichenbach, A., Liebert, U.G., Illes, P., 2005. P2X(7) receptor-mRNA and -protein in the mouse retina; changes during retinal degeneration in BALB/c mice. *Neurochem. Int.* 47, 235–242.
- Galindo-Romero, C., Aviles-Trigueros, M., Jimenez-Lopez, M., Valiente-Soriano, F.J., Salinas-Navarro, M., Nadal-Nicolas, F., Villegas-Perez, M.P., Vidal-Sanz, M., Agudo-Barriso, M., 2011. Axotomy-induced retinal ganglion cell death in adult mice: quantitative and topographic time course analyses. *Exp. Eye Res.* 92, 377–387.
- Goyal, A., Srivastava, A., Sihota, R., Kaur, J., 2014. Evaluation of oxidative stress markers in aqueous humor of primary open angle glaucoma and primary angle closure glaucoma patients. *Curr. Eye Res.* 39, 823–829.
- Harada, C., Nakamura, K., Namekata, K., Okumura, A., Mitamura, Y., Iizuka, Y., Kashiwagi, K., Yoshida, K., Ohno, S., Matsuzawa, A., Tanaka, K., Ichijo, H., Harada, T., 2006. Role of apoptosis signal-regulating kinase 1 in stress-induced neural cell apoptosis in vivo. *Am. J. Pathol.* 168, 261–269.
- Harder, J.M., Fernandes, K.A., Libby, R.T., 2012. The Bcl-2 family member BIM has multiple glaucoma-relevant functions in DBA/2J mice. *Sci. Rep.* 2, 530.
- Heiduschka, P., Julien, S., Schuettauf, F., Schnichels, S., 2010. Loss of retinal function in aged DBA/2J mice - New insights into retinal neurodegeneration. *Exp. Eye Res.* 91, 779–783.
- Howell, G.R., Libby, R.T., Marchant, J.K., Wilson, L.A., Cosma, I.M., Smith, R.S., Anderson, M.G., John, S.W., 2007. Absence of glaucoma in DBA/2J mice homozygous for wild-type versions of Gpnmb and Tyrp1. *BMC Genet.* 8, 45.
- Hu, H., Lu, W., Zhang, M., Zhang, X., Argall, A.J., Patel, S., Lee, G.E., Kim, Y.C., Jacobson, K.A., Laties, A.M., Mitchell, C.H., 2010. Stimulation of the P2X7 receptor kills rat retinal ganglion cells in vivo. *Exp. Eye Res.* 91, 425–432.
- Inman, D.M., Sappington, R.M., Horner, P.J., Calkins, D.J., 2006. Quantitative correlation of optic nerve pathology with ocular pressure and corneal thickness in the DBA/2 mouse model of glaucoma. *Invest. Ophthalmol. Vis. Sci.* 47, 986–996.
- Ishii, K., Kaneda, M., Li, H., Rockland, K.S., Hashikawa, T., 2003. Neuron-specific distribution of P2X7 purinergic receptors in the monkey retina. *J. Comp. Neurol.* 459, 267–277.
- Jakobs, T.C., Libby, R.T., Ben, Y., John, S.W., Masland, R.H., 2005. Retinal ganglion cell degeneration is topological but not cell type specific in DBA/2J mice. *J. Cell Biol.* 171, 313–325.
- Jimenez-Pacheco, A., Mesuret, G., Sanz-Rodriguez, A., Tanaka, K., Mooney, C., Conroy, R., Miras-Portugal, M.T., Diaz-Hernandez, M., Henschall, D.C., Engel, T., 2013. Increased neocortical expression of the P2X7 receptor after status epilepticus and anticonvulsant effect of P2X7 receptor antagonist A-438079. *Epilepsia* 54, 1551–1561.
- John, S.W., Smith, R.S., Savinova, O.V., Hawes, N.L., Chang, B., Turnbull, D., Davisson, M., Roderick, T.H., Heckenlively, J.R., 1998. Essential iris atrophy, pigment dispersion, and glaucoma in DBA/2J mice. *Invest. Ophthalmol. Vis. Sci.* 39, 951–962.
- Johnson, E.C., Guo, Y., Cepurna, W.O., Morrison, J.C., 2009. Neurotrophin roles in retinal ganglion cell survival: lessons from rat glaucoma models. *Exp. Eye Res.* 88, 808–815.
- Jun, D.J., Kim, J., Jung, S.Y., Song, R., Noh, J.H., Park, Y.S., Ryu, S.H., Kim, J.H., Kong, Y.Y., Chung, J.M., Kim, K.T., 2007. Extracellular ATP mediates necrotic cell swelling in SN4741 dopaminergic neurons through P2X7 receptors. *J. Biol. Chem.* 282, 37350–37358.
- Kerrigan, L.A., Zack, D.J., Quigley, H.A., Smith, S.D., Pease, M.E., 1997. TUNEL-positive ganglion cells in human primary open-angle glaucoma. *Arch. Ophthalmol.* 115, 1031–1035.
- Kikuchi, M., Tenneti, L., Lipton, S.A., 2000. Role of p38 mitogen-activated protein kinase in axotomy-induced apoptosis of rat retinal ganglion cells. *J. Neurosci.* 20, 5037–5044.
- Kim, H.S., Park, C.K., 2005. Retinal ganglion cell death is delayed by activation of retinal intrinsic cell survival program. *Brain Res.* 1057, 17–28.
- Ko, M.L., Hu, D.N., Ritch, R., Sharma, S.C., 2000. The combined effect of brain-derived neurotrophic factor and a free radical scavenger in experimental glaucoma. *Invest. Ophthalmol. Vis. Sci.* 41, 2967–2971.
- Kong, Q., Wang, M., Liao, Z., Camden, J.M., Yu, S., Simonyi, A., Sun, G.Y., Gonzalez, F.A., Erb, L., Seye, C.I., Weisman, G.A., 2005. P2X(7) nucleotide receptors mediate caspase-8/9/3-dependent apoptosis in rat primary cortical neurons. *Purinergic Signal.* 1, 337–347.
- Levkovitch-Verbin, H., 2015. Retinal ganglion cell apoptotic pathway in glaucoma: initiating and downstream mechanisms. *Prog. Brain Res.* 220, 37–57.
- Levkovitch-Verbin, H., Quigley, H.A., Martin, K.R., Harizman, N., Valenta, D.F., Pease, M.E., Melamed, S., 2005. The transcription factor c-jun is activated in retinal ganglion cells in experimental rat glaucoma. *Exp. Eye Res.* 80, 663–670.
- Levkovitch-Verbin, H., Harizman, N., Dardik, R., Nisgav, Y., Vander, S., Melamed, S., 2007. Regulation of cell death and survival pathways in experimental glaucoma. *Exp. Eye Res.* 85, 250–258.
- Levkovitch-Verbin, H., Makarovsky, D., Vander, S., 2013. Comparison between axonal and retinal ganglion cell gene expression in various optic nerve injuries including glaucoma. *Mol. Vis.* 19, 2526–2541.
- Li, A., Zhang, X., Zheng, D., Ge, J., Laties, A.M., Mitchell, C.H., 2011. Sustained elevation of extracellular ATP in aqueous humor from humans with primary chronic angle-closure glaucoma. *Exp. Eye Res.* 93, 528–533.
- Libby, R.T., Anderson, M.G., Pang, I.H., Robinson, Z.H., Savinova, O.V., Cosma, I.M., Snow, A., Wilson, L.A., Smith, R.S., Clark, A.F., John, S.W., 2005. Inherited glaucoma in DBA/2J mice: pertinent disease features for studying the neurodegeneration. *Vis. Neurosci.* 22, 637–648.
- Lindqvist, N., Peinado-Ramonn, P., Vidal-Sanz, M., Hallbook, F., 2004. GDNF, Ret, GFRalpha1 and 2 in the adult rat retino-tectal system after optic nerve transection. *Exp. Neurol.* 187, 487–499.
- Manabe, S., Lipton, S.A., 2003. Divergent NMDA signals leading to proapoptotic and antiapoptotic pathways in the rat retina. *Invest. Ophthalmol. Vis. Sci.* 44, 385–392.
- Mangiarini, L., Sathasivam, K., Seller, M., Cozens, B., Harper, A., Hetherington, C., Lawton, M., Trotter, Y., Leach, H., Davies, S.W., Bates, G.P., 1996. Exon 1 of the HD gene with an expanded CAG repeat is sufficient to cause a progressive neurological phenotype in transgenic mice. *Cell* 87, 493–506.
- McElnea, E.M., Quill, B., Docherty, N.G., Irnaten, M., Siah, W.F., Clark, A.F., O'Brien, C.J., Wallace, D.M., 2011. Oxidative stress, mitochondrial dysfunction and calcium overload in human lamina cribrosa cells from glaucoma donors. *Mol. Vis.* 17, 1182–1191.
- McKinnon, S.J., Schlamp, C.L., Nickells, R.W., 2009. Mouse models of retinal ganglion cell death and glaucoma. *Exp. Eye Res.* 88, 816–824.
- Mitchell, C.H., Lu, W., Hu, H., Zhang, X., Reigada, D., Zhang, M., 2009. The P2X(7) receptor in retinal ganglion cells: a neuronal model of pressure-induced damage and protection by a shifting purinergic balance. *Purinergic Signal.* 5, 241–249.
- Monif, M., Burnstock, G., Williams, D.A., 2010. Microglia: proliferation and activation driven by the P2X7 receptor. *Int. J. Biochem. Cell Biol.* 42, 1753–1756.
- Montalban-Soler, L., Alarcon-Martinez, L., Jimenez-Lopez, M., Salinas-Navarro, M., Galindo-Romero, C., Bezerra de Sa, F., Garcia-Ayuso, D., Aviles-Trigueros, M., Vidal-Sanz, M., Agudo-Barriso, M., Villegas-Perez, M.P., 2012. Retinal compensatory changes after light damage in albino mice. *Mol. Vis.* 18, 675–693.
- Morrison, J.C., Moore, C.G., Deppmeier, L.M., Gold, B.G., Meshul, C.K., Johnson, E.C., 1997. A rat model of chronic pressure-induced optic nerve damage. *Exp. Eye Res.* 64, 85–96.
- Munemasa, Y., Ohtani-Kaneko, R., Kitaoka, Y., Kuribayashi, K., Isenoumi, K., Kogo, J., Yamashita, K., Kumai, T., Kobayashi, S., Hirata, K., Ueno, S., 2005. Contribution of mitogen-activated protein kinases to NMDA-induced neurotoxicity in the rat retina. *Brain Res.* 1044, 227–240.
- Munemasa, Y., Ohtani-Kaneko, R., Kitaoka, Y., Kumai, T., Kitaoka, Y., Hayashi, Y., Watanabe, M., Takeda, H., Hirata, K., Ueno, S., 2006. Pro-apoptotic role of c-Jun in NMDA-induced neurotoxicity in the rat retina. *J. Neurosci. Res.* 83, 907–918.
- Nadal-Nicolas, F.M., Jimenez-Lopez, M., Sobrado-Calvo, P., Nieto-Lopez, L., Canovas-Martinez, I., Salinas-Navarro, M., Vidal-Sanz, M., Agudo, M., 2009. Brn3a as a marker of retinal ganglion cells: qualitative and quantitative time course studies in naive and optic nerve-injured retinas. *Invest. Ophthalmol. Vis. Sci.* 50, 3860–3868.
- Nagaraju, M., Saleh, M., Porciatti, V., 2007. IOP-dependent retinal ganglion cell dysfunction in glaucomatous DBA/2J mice. *Invest. Ophthalmol. Vis. Sci.* 48, 4573–4579.
- Nassar, K., Tura, A., Luke, J., Luke, M., Grisanti, S., Grisanti, S., 2015. A p38 MAPK inhibitor improves outcome after Glaucoma filtration surgery. *J. Glaucoma* 24, 165–178.
- Niyadurupola, N., Sidaway, P., Ma, N., Rhodes, J.D., Broadway, D.C., Sanderson, J., 2013.

- P2X7 receptor activation mediates retinal ganglion cell death in a human retina model of ischemic neurodegeneration. *Invest. Ophthalmol. Vis. Sci.* 54, 2163–2170.
- Okisaka, S., Murakami, A., Mizukawa, A., Ito, J., 1997. Apoptosis in retinal ganglion cell decrease in human glaucomatous eyes. *Jpn. J. Ophthalmol.* 41, 84–88.
- Ono, K., Han, J., 2000. The p38 signal transduction pathway: activation and function. *Cell. Signal.* 12, 1–13.
- Pananka, W., Jijon, H., Herx, L.M., Armstrong, J.N., Feighan, D., Wei, T., Yong, V.W., Ransohoff, R.M., MacVicar, B.A., 2001. P2X7-like receptor activation in astrocytes increases chemokine monocyte chemoattractant protein-1 expression via mitogen-activated protein kinase. *J. Neurosci.* 21, 7135–7142.
- Pannicke, T., Fischer, W., Biedermann, B., Schadlich, H., Grosche, J., Faude, F., Wiedemann, P., Allgaier, C., Illes, P., Burnstock, G., Reichenbach, A., 2000. P2X7 receptors in Muller glial cells from the human retina. *J. Neurosci.* 20, 5965–5972.
- Parrilla-Reverter, G., Agudo, M., Nadal-Nicolas, F., Alarcon-Martinez, L., Jimenez-Lopez, M., Salinas-Navarro, M., Sobrado-Calvo, P., Bernal-Garro, J.M., Villegas-Perez, M.P., Vidal-Sanz, M., 2009. Time-course of the retinal nerve fibre layer degeneration after complete intra-orbital optic nerve transection or crush: a comparative study. *Vision Res.* 49, 2808–2825.
- Perez de Lara, M.J., Santano, C., Guzman-Aranguez, A., Valiente-Soriano, F.J., Aviles-Trigueros, M., Vidal-Sanz, M., de la Villa, P., Pintor, J., 2014. Assessment of inner retina dysfunction and progressive ganglion cell loss in a mouse model of glaucoma. *Exp. Eye Res.* 122, 40–49.
- Perez de Lara, M.J., Guzman-Aranguez, A., de la Villa, P., Diaz-Hernandez, J.I., Miras-Portugal, M.T., Pintor, J., 2015. Increased levels of extracellular ATP in glaucomatous retinas: possible role of the vesicular nucleotide transporter during the development of the pathology. *Mol. Vis.* 21, 1060–1070.
- Perez de Lara, M.J., Guzman-Aranguez, A., Gomez-Villafuertes, R., Gualix, J., Miras-Portugal, M.T., Pintor, J., 2018. Increased Ap4A levels and ecto-nucleotidase activity in glaucomatous mouse retina. *Purinergic Signal.*
- Puthussery, T., Fletcher, E.L., 2004. Synaptic localization of P2X7 receptors in the rat retina. *J. Comp. Neurol.* 472, 13–23.
- Puthussery, T., Fletcher, E., 2009. Extracellular ATP induces retinal photoreceptor apoptosis through activation of purinoceptors in rodents. *J. Comp. Neurol.* 513, 430–440.
- Puthussery, T., Yee, P., Vingrys, A.J., Fletcher, E.L., 2006. Evidence for the involvement of purinergic P2X receptors in outer retinal processing. *Eur. J. Neurosci.* 24, 7–19.
- Quigley, H.A., Broman, A.T., 2006. The number of people with glaucoma worldwide in 2010 and 2020. *Br. J. Ophthalmol.* 90, 262–267.
- Reichstein, D., Ren, L., Filippopoulos, T., Mittag, T., Danias, J., 2007. Apoptotic retinal ganglion cell death in the DBA/2J mouse model of glaucoma. *Exp. Eye Res.* 84, 13–21.
- Reigada, D., Lu, W., Zhang, M., Mitchell, C.H., 2008. Elevated pressure triggers a physiological release of ATP from the retina: possible role for pannexin hemichannels. *Neuroscience* 157, 396–404.
- Resta, V., Novelli, E., Di Virgilio, F., Galli-Resta, L., 2005. Neuronal death induced by endogenous extracellular ATP in retinal cholinergic neuron density control. *Development* 132, 2873–2882.
- Resta, V., Novelli, E., Vozzi, G., Scarpa, C., Caleo, M., Ahluwalia, A., Solini, A., Santini, E., Parisi, V., Di Virgilio, F., Galli-Resta, L., 2007. Acute retinal ganglion cell injury caused by intraocular pressure spikes is mediated by endogenous extracellular ATP. *Eur. J. Neurosci.* 25, 2741–2754.
- Roth, S., Shaikh, A.R., Hennelly, M.M., Li, Q., Bindokas, V., Graham, C.E., 2003. Mitogen-activated protein kinases and retinal ischemia. *Invest. Ophthalmol. Vis. Sci.* 44, 5383–5395.
- Saleh, M., Nagaraju, M., Porciatti, V., 2007. Longitudinal evaluation of retinal ganglion cell function and IOP in the DBA/2J mouse model of glaucoma. *Invest. Ophthalmol. Vis. Sci.* 48, 4564–4572.
- Salinas-Navarro, M., Alarcon-Martinez, L., Valiente-Soriano, F.J., Ortin-Martinez, A., Jimenez-Lopez, M., Aviles-Trigueros, M., Villegas-Perez, M.P., de la Villa, P., Vidal-Sanz, M., 2009. Functional and morphological effects of laser-induced ocular hypertension in retinas of adult albino Swiss mice. *Mol. Vis.* 15, 2578–2598.
- Salinas-Navarro, M., Alarcon-Martinez, L., Valiente-Soriano, F.J., Jimenez-Lopez, M., Mayor-Torrogosa, S., Aviles-Trigueros, M., Villegas-Perez, M.P., Vidal-Sanz, M., 2010. Ocular hypertension impairs optic nerve axonal transport leading to progressive retinal ganglion cell degeneration. *Exp. Eye Res.* 90, 168–183.
- Sanchez-Migallon, M.C., Valiente-Soriano, F.J., Nadal-Nicolas, F.M., Vidal-Sanz, M., Agudo-Barriuso, M., 2016. Apoptotic retinal ganglion cell death after optic nerve transection or crush in mice: delayed RGC loss with BDNF or a caspase 3 inhibitor. *Invest. Ophthalmol. Vis. Sci.* 57, 81–93.
- Sanchez-Migallon, M.C., Valiente-Soriano, F.J., Salinas-Navarro, M., Nadal-Nicolas, F.M., Jimenez-Lopez, M., Vidal-Sanz, M., Agudo-Barriuso, M., 2018. Nerve fibre layer degeneration and retinal ganglion cell loss long term after optic nerve crush or transection in adult mice. *Exp. Eye Res.* 170, 40–50.
- Sanchez-Nogueiro, J., Marin-Garcia, P., Miras-Portugal, M.T., 2005. Characterization of a functional P2X(7)-like receptor in cerebellar granule neurons from P2X(7) knockout mice. *FEBS Lett.* 579, 3783–3788.
- Sawada, A., Neufeld, A.H., 1999. Confirmation of the rat model of chronic, moderately elevated intraocular pressure. *Exp. Eye Res.* 69, 525–531.
- Schlamp, C.L., Li, Y., Dietz, J.A., Janssen, K.T., Nickells, R.W., 2006. Progressive ganglion cell loss and optic nerve degeneration in DBA/2J mice is variable and asymmetric. *BMC Neurosci.* 7, 66.
- Schneider, C.A., Rasband, W.S., Eliceiri, K.W., 2012. NIH Image to ImageJ: 25 years of image analysis. *Nat. Methods* 9, 671–675.
- Schuettauf, F., Rejda, R., Walski, M., Frontczak-Baniewicz, M., Voelker, M., Blatsios, G., Shinoda, K., Zagorski, Z., Zrenner, E., Grieb, P., 2004. Retinal neurodegeneration in the DBA/2J mouse—a model for ocular hypertension. *Acta Neuropathol.* 107, 352–358.
- Skaper, S.D., Debetto, P., Giusti, P., 2010. The P2X7 purinergic receptor: from physiology to neurological disorders. *FASEB J.* 24, 337–345.
- Smith, B.J., Wang, X., Chauhan, B.C., Cote, P.D., Tremblay, F., 2014. Contribution of retinal ganglion cells to the mouse electroretinogram. *Doc. Ophthalmol.* 128, 155–168.
- Sugiyama, T., Kobayashi, M., Kawamura, H., Li, Q., Puro, D.G., 2004. Enhancement of P2X(7)-induced pore formation and apoptosis: an early effect of diabetes on the retinal microvasculature. *Invest. Ophthalmol. Vis. Sci.* 45, 1026–1032.
- Sugiyama, T., Kawamura, H., Yamanishi, S., Kobayashi, M., Katsumura, K., Puro, D.G., 2005. Regulation of P2X7-induced pore formation and cell death in pericyte-containing retinal microvessels. *Am. J. Physiol., Cell Physiol.* 288, C568–576.
- Sugiyama, T., Oku, H., Shibata, M., Fukuhara, M., Yoshida, H., Ikeda, T., 2010. Involvement of P2X7 receptors in the hypoxia-induced death of rat retinal neurons. *Invest. Ophthalmol. Vis. Sci.* 51, 3236–3243.
- Sugiyama, T., Lee, S.Y., Horie, T., Oku, H., Takai, S., Tanioka, H., Kuriki, Y., Kojima, S., Ikeda, T., 2013. P2X(7) receptor activation may be involved in neuronal loss in the retinal ganglion cell layer after acute elevation of intraocular pressure in rats. *Mol. Vis.* 19, 2080–2091.
- Surprenant, A., Rassendren, F., Kawashima, E., North, R.A., Buell, G., 1996. The cytolytic P2Z receptor for extracellular ATP identified as a P2X receptor (P2X7). *Science* 272, 735–738.
- Suzuki, T., Hide, I., Ido, K., Kohsaka, S., Inoue, K., Nakata, Y., 2004. Production and release of neuroprotective tumor necrosis factor by P2X7 receptor-activated microglia. *J. Neurosci.* 24, 1–7.
- Tatton, N.A., Tezel, G., Insolia, S.A., Nandor, S.A., Edward, P.D., Wax, M.B., 2001. In situ detection of apoptosis in normal pressure glaucoma. A preliminary examination. *Surv. Ophthalmol.* 45 (Suppl 3), S268–272 discussion S273–266.
- Tezel, G., 2006. Oxidative stress in glaucomatous neurodegeneration: mechanisms and consequences. *Prog. Retin. Eye Res.* 25, 490–513.
- Tezel, G., Chauhan, B.C., LeBlanc, R.P., Wax, M.B., 2003. Immunohistochemical assessment of the glial mitogen-activated protein kinase activation in glaucoma. *Invest. Ophthalmol. Vis. Sci.* 44, 3025–3033.
- Valiente-Soriano, F.J., Salinas-Navarro, M., Jimenez-Lopez, M., Alarcon-Martinez, L., Ortin-Martinez, A., Bernal-Garro, J.M., Aviles-Trigueros, M., Agudo-Barriuso, M., Villegas-Perez, M.P., Vidal-Sanz, M., 2015. Effects of ocular hypertension in the visual system of pigmented mice. *PLoS One* 10, e0121134.
- Vessey, K.A., Fletcher, E.L., 2012. Rod and cone pathway signalling is altered in the P2X7 receptor knock out mouse. *PLoS One* 7, e29990.
- Vidal-Sanz, M., Valiente-Soriano, F.J., Ortin-Martinez, A., Nadal-Nicolas, F.M., Jimenez-Lopez, M., Salinas-Navarro, M., Alarcon-Martinez, L., Garcia-Ayuso, D., Aviles-Trigueros, M., Agudo-Barriuso, M., Villegas-Perez, M.P., 2015. Retinal neurodegeneration in experimental glaucoma. *Prog. Brain Res.* 220, 1–35.
- Vidal-Sanz, M., Galindo-Romero, C., Valiente-Soriano, F.J., Nadal-Nicolas, F.M., Ortin-Martinez, A., Rovere, G., Salinas-Navarro, M., Lucas-Ruiz, F., Sanchez-Migallon, M.C., Sobrado-Calvo, P., Aviles-Trigueros, M., Villegas-Perez, M.P., Agudo-Barriuso, M., 2017. Shared and differential retinal responses against optic nerve injury and ocular hypertension. *Front. Neurosci.* 11, 235.
- Wang, C.M., Chang, Y.Y., Sun, S.H., 2003. Activation of P2X7 purinoceptor-stimulated TGF-beta 1 mRNA expression involves PKC/MAPK signalling pathway in a rat brain-derived type-2 astrocyte cell line, RBA-2. *Cell. Signal.* 15, 1129–1137.
- Weisman, G.A., Camden, J.M., Peterson, T.S., Ajit, D., Woods, L.T., Erb, L., 2012. P2 receptors for extracellular nucleotides in the central nervous system: role of P2X7 and P2Y(2) receptor interactions in neuroinflammation. *Mol. Neurobiol.* 46, 96–113.
- Wheeler-Schilling, T.H., Marquardt, K., Kohler, K., Guenther, E., Jabs, R., 2001. Identification of purinergic receptors in retinal ganglion cells. *Brain Res. Mol. Brain Res.* 92, 177–180.
- Xia, J., Lim, J.C., Lu, W., Beckel, J.M., Macarak, E.J., Laties, A.M., Mitchell, C.H., 2012. Neurons respond directly to mechanical deformation with pannexin-mediated ATP release and autostimulation of P2X7 receptors. *J. Physiol. (Lond.)* 590, 2285–2304.
- Zhang, X., Zhang, M., Laties, A.M., Mitchell, C.H., 2005. Stimulation of P2X7 receptors elevates Ca²⁺ and kills retinal ganglion cells. *Invest. Ophthalmol. Vis. Sci.* 46, 2183–2191.
- Zhang, X., Li, A., Ge, J., Reigada, D., Laties, A.M., Mitchell, C.H., 2007. Acute increase of intraocular pressure releases ATP into the anterior chamber. *Exp. Eye Res.* 85, 637–643.
- Zhou, X., Li, F., Kong, L., Tomita, H., Li, C., Cao, W., 2005. Involvement of inflammation, degradation, and apoptosis in a mouse model of glaucoma. *J. Biol. Chem.* 280, 31240–31248.